A box-model of carrying capacity of the Thau lagoon in the context of ecological status regulations and sustainable shellfish cultures

Romain Pete, Thomas Guyondet, Beatrice Bec, Valerie Derolez, Ludovic Cesmat, Franck Lagarde, Stéphane Pouvreau, Annie Fiandrino, Marion Richard

Tittle: A box-model of carrying capacity of the Thau lagoon in the context of ecological status regulations and sustainable shellfish cultures.

Authors: Romain Pete[1], Thomas Guyondet[2], Beatrice Bec[1], Valérie Derolez[1], Ludovic Cesmat[3], Franck Lagarde[1], Stéphane Pouvreau[4], Annie Fiandrino[1], Marion Richard[1]

1 Marine Biodiversity, Exploitation and Conservation (MARBEC). Univ Montpellier, CNRS, Ifremer, IRD, Montpellier & Sète, France

2 Department of Fisheries and Oceans, Gulf Fisheries Center, P.O. Box 5030, Science Branch, Moncton, Canada NB E1C 9B6

3 Syndicat Mixte du Bassin de Thau, 328, Quai des Moulins-34200 SETE

4 Ifremer, Laboratoire des Sciences de l'Environnement Marin (LEMAR), 29840 Argenton-en-Landunvez, France

Corresponding author :
Dr. Romain Pete
MARBEC, CC093, Place Eugène Bataillon, 34095, Montpellier Cedex 5, France.
Romain.Pete@umontpellier.fr

Abstract:

The decrease of microbial and nutrient inputs from the watershed has long dominated lagoon ecosystem management objectives. Phytoplankton biomass and abundance have drastically decreased for more than a decade and *Zostera* meadow have gradually recovered, expressing lagoon ecosystem restoration such as Thau lagoon. Do the progressive achievement of the good ecological status of the Thau lagoon possibly threatens the shellfish industry in terms of production and oyster quality, by reducing the carrying capacity? To provide answers about the right balance to be achieved between conservation and exploitation, a new numerical tool was developed to help in decision-making. We hereby propose to incorporate a Dynamic Energy Budget type shellfish production model to an existing lagoon ecosystem box-model. The influence of different scenarios of nutrient inputs (related to projections of population growth or improvement of treatment plants) and shellfish stocks were tested on oyster performances (production, oyster condition index), carrying capacity of the lagoon and ecological status indices used within the EU Water Framework Directive. Model outputs demonstrated that shellfish production was mainly controlled by nutrient inputs, which depend on hydro-meteorological variability, and specifically by phosphorus and N:P ratios of nutrient inputs. Scenarios tested, however, demonstrated smaller differences of oyster production in comparison to inter-annual variability. The overall ecological status of the lagoon remained in a "good" status with acceptable lagoon-scale phytoplankton depletion, regardless of scenarios, setting the carrying capacity of this ecosystem to be sustainable.

Key words: shellfish farming, carrying capacity, stakeholder implication, nitrogen and phosphorus inputs, Water Frame Directive, ecological indicators, phytoplankton depletion, coupled Biogeochemical-DEB model.

1 Introduction

Rapid expansion of bivalve aquaculture in the last few decades with 17.1 million tons of mollusks produced worldwide (FAO, 2018) plays a key role in local socio-economic developments. FAO therefore promoted, in its recent report, a holistic and integrated ecosystem approach of aquaculture (EAA) to address management issues of sustainable aquaculture. Among the key features of this EEA framework, FAO highlighted: the wide stakeholder participation in planning and implementing; a comprehensive consideration of major components, e.g. aquaculture, socio-economics and environmental, based on "best available knowledge"; and a search for a trade-off between environment/conservation and socio-economic objectives. This rapid growing economic sector has inevitably raised questions of carrying capacity and sustainability (Nunes et al., 2003).

In this context, the concept of the carrying capacity is commonly used as it involves major aspects of integrated ecosystem functioning such as physics, productivity, ecology and socio-economics (McKindsey et al., 2006). Regarding cultured bivalves, this carrying capacity can be primarily defined as the biomass of a population supported permanently by a given system (Dame and Prins., 1998; Kashiwai, 1998). However, this definition has been successively extended to a maximized production without affecting growth rates (Carver and Mallet, 1990) to a maximized production of marketable cohorts (Bacher et al., 1998) and more recently to a maximized production within the frame of environmental sustainability (Smaal et al., 1997; Ferreira et al., 2008; Byron et al., 2011b; Filgueira et al., 2015). The current consensus is that production carrying capacity represents the stock that maximizes harvests while ecosystem responses or ecological carrying capacity deal with unwanted modifications of phytoplankton abundances, nutrient cycling or organic content in sediments (McKindsey et al., 2006; Grant et al., 2007; Guyondet et al., 2014;).

Recent research has been promoting use of mathematical models, of various complexity (Dabrowski et al., 2013), to tackle the issues of cultured shellfish management. A lot of efforts have been made in the representation of shellfish modeling from individual based (Gangnery, 2003) to mechanistic (Bourlès et al., 2009; Kooijman, 2010; Alunno-Bruscia et al., 2011) and mixed (Brigolin et al., 2009) models. These individual models are then coupled to ecosystem food web-based models that include most of the relevant biological compartments of aquatic systems (Grangeré et al., 2009; Byron et al., 2011c; Filgueira et al., 2014b). These coupled models can thus be complexified by representing exchanges with the outer world through simple renewal times (Grangeré et al., 2009), box-model (Chapelle et al., 2000; Filgueira and Grant, 2009; Raillard and Menesguen, 1994) and fully spatialized hydrodynamic models (Guyondet et al., 2010). While these models give insights into the carrying capacity of an ecosystem, it is crucial to derive other model outputs to evaluate impacts of shellfish farming on ecosystem functioning.

The Thau lagoon, as many other coastal Mediterranean lagoons, has been experiencing major anthropogenic pressures as it received large nutrient loadings from its watershed (La Jeunesse and Elliott, 2004; Plus et al., 2006). These nutrient inputs have been identified as the main cause of eutrophication issues or dystrophic crisis (Souchu et al., 1998; Harzallah and Chapelle, 2002). Thus, many efforts have been made to reduce nutrient loadings mainly through the installation of waste water treatment plants (WWTP) in the 1970's and their refurbishment later in the 2000's. These works have drastically reduced the amount of nutrient inputs from the watershed and successfully led to reach a current "good" ecological status of water column of the Thau lagoon according to the EU Water Framework Directive (WFD) (EC, 2000; Derolez et al, 2019). These profound changes in the lagoon inputs from the watershed have raised concerns from shellfish farmers. Oyster farming, after having taken precedence over mussel farming in the 1990s, has seen its activity largely impacted by

juvenile mortality phenomena from 2008 (Pernet et al., 2012) , which significantly reduced the overall annual shellfish production. Under current production conditions, long-term observations of farmed oyster performances have shown improved growth rates and condition index, probably linked to a decrease in the oyster stock, despite the decrease in phytoplankton biomass observed (Bec et al., 2018). Considering these recent and important changes in the pressures exerted on the Thau lagoon, an assessment of its ecological carrying capacity for shellfish culture is required. We hereby present a modelling work to address concerns arising from shellfish farmers and consider realistic actions combining the achievement of regulatory constraints and the sustainability of this major socio-economic activity.

The GAMELag model (Pete et al, *tbs*) was formerly developed for the Bages-Sigean lagoon, to produce similar ecological indicators as those used in the WFD (European Community, 2000). These indicators have been established as relevant criterion to assess ecological status of a given ecosystem according to different categories from “high” to “very bad”. In addition, a dynamic energy budget (DEB) model for the Pacific oyster *Crassostrea gigas*, formerly developed on the Atlantic coast (Pouvreau et al., 2006; Bernard et al., 2011a), was parameterized for the Thau lagoon and coupled to the GAMELag model. Concomitantly to the model implementation, a major part of the presented work was realized in close partnership with shellfish growers, local and governmental management bodies and scientists. Based on this joint work, management scenarios were established on realistic working hypotheses. The objectives of this work were therefore: 1) to build a carrying capacity model and 2) to test the effects of nitrogen and phosphorus inputs and oyster stocking densities, on oyster performances (condition index, production), carrying capacity and ecological status of the Thau lagoon. This work was carried out in collaboration with managers and farmers to find the right balance between conservation and exploitation for sustainable development of shellfish farming in good ecological status coastal area.

2 Material & Methods

2.1 Study site

Thau lagoon (Figure 1) is located on the south coast of France (43.18'- 43.28'N, 3.30'-3.45'E) and has a total area of 68 km^2 (19,5km long by 4.5 km width) and an average depth of 4 m (Fiandrino et al., 2017). The lagoon is connected to the sea through two inlets, i.e., the Sète channel in the north (90% of sea water exchanges) and the Grau de Pisse-Saumes inlet in the south. The Sète channel is 2.4 km long with a mean cross-section of about 300 m^2. The Mediterranean climate is characterised by a wide range of temperatures (5–29 °C) and salinities in the lagoon cover a range of 27–42 with a low spatial gradient (data from REPHY monitoring network; Fiandrino et al., 2017).

The lagoon has a narrow located between the Balaruc Point and the Barrou Point, separating the lagoon into two basins, the "Petit Etang" to the East and "Grand Etang" to the West. The Grand Etang is the location of shellfish farming activities spread over three areas at the north of this basin (20% of the lagoon surface). These shellfish farming zones, namely Bouzigues, Mèze and Marseillan (Figure 1), gather around 2800 farming structures (1250 m^2 and a total area of ~640 ha) harbouring growing oyster juveniles (hereafter spat) and adults (hereafter oyster) of the pacific oyster *Crassostrea gigas* (70% of the shellfish stocks) and mussel *Mytilus galloprovincialis*.

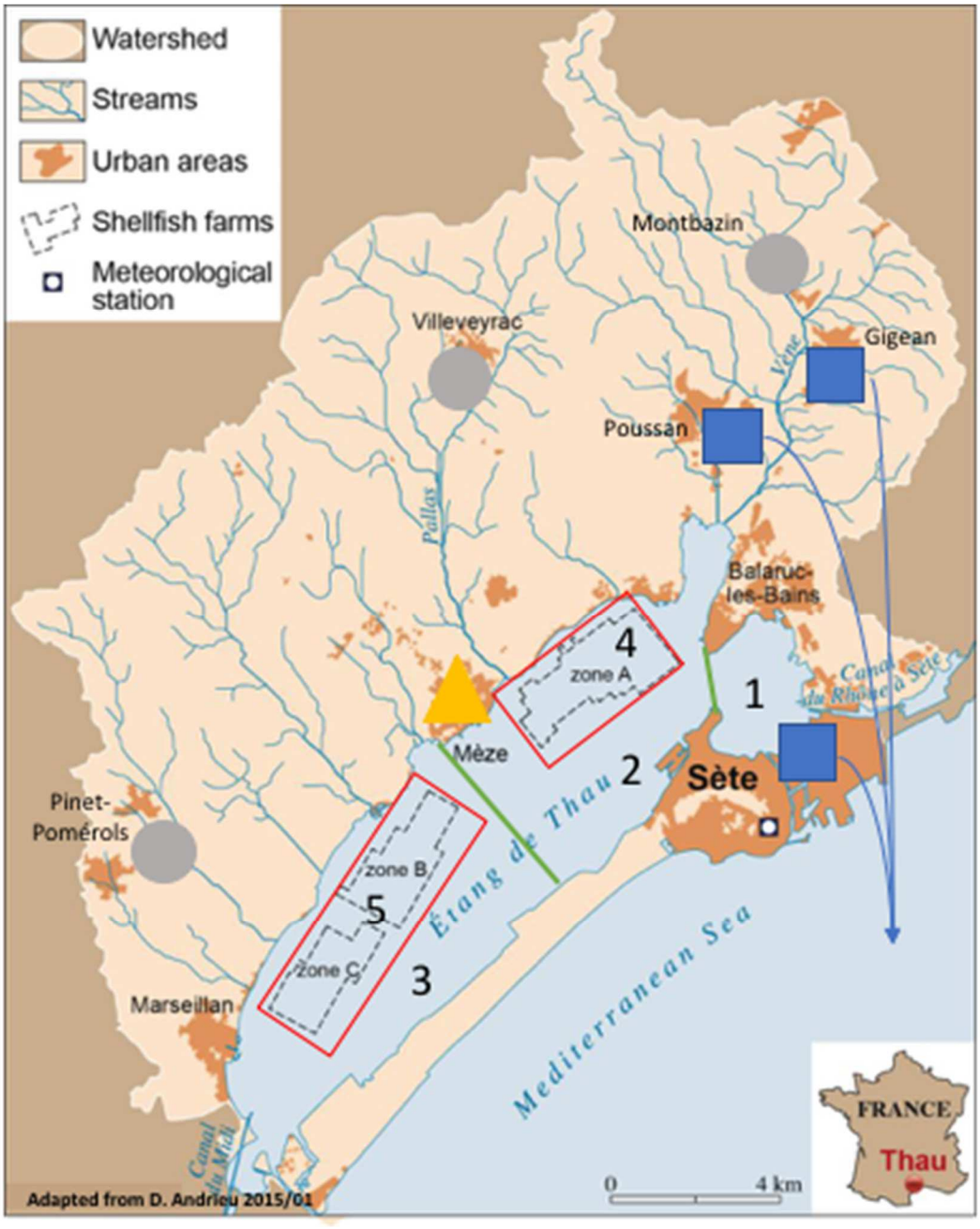

Figure 1. Map of the Thau lagoon and its watershed. WWTP are located by symbols and distinguish WWTP releasing to the sea (squares), using normal abatements (circles) or maximum abatements (triangle). Hydrodynamic frontiers are represented by green lines separating three basins (numbered 1 to 3) and shellfish farming area are located by the two red boxes (numbered 4 and 5).

The watershed spreads mainly northward from the lagoon over an area of 280 km^2 and is drained by several rivers with intermittent flows. The main tributary (the Vène River) is connected to the Crique de l'Angle area and brings an annual average of 15.1 Mm^3 of

128 freshwater (about 50% of total flow, ranging from 3.1 to 24.7 Mm^3 between 2009 and 2016).
129 The population in this watershed amounts to 126604 inhabitants (French National Institute of
130 Statistics and Economical Studies, Insee, 2015) over 14 main cities equipped with waste
131 water treatment plants (WWTP). Five of these towns, Sète, Poussan, Bouzigues, Gigean and
132 Balaruc (Figure 1) are connected to the Sète WWTP which discards effluents 7 km offshore
133 in the Mediterranean Sea. The four other cities, Montbazin, Villeveyrac, Mèze-Loupian and
134 Pinet-Pomerols have their own WWTP releasing effluents into the Thau lagoon.
135
136 2.2 Carrying capacity model
137 The GAMELag model (Pete et al, *tbs*) was formerly developed for management purposes
138 with regards to water quality assessment under the WFD. GAMELag works on the principle
139 of a box-model, where the lagoon is represented by basins, physically homogeneous, in which
140 the stocks of the different biological compartments are simulated as well as the fluxes of
141 matter (nitrogen N and phosphorus P) connecting these compartments (Figure 2). The lagoon
142 was separated into three main boxes (green boxes, Fig. 1): "Petit Etang" (box 1), East of
143 "Grand Etang" and West of "Grand Etang" (box 2 and 3, respectively on Fig. 1). In order to
144 simplify the model and to be able to compare it with available observations, the Mèze and
145 Marseillan shellfish farming zones were gathered to form box 5, whereas Bouzigues shellfish
146 farming zone formed box 4 (red boxes, Fig. 1).
147 The hydrodynamic exchanges between box 1 and the Mediterranean Sea and between two
148 adjacent physical boxes are simulated following formalism defined by Gordon et al, 1996
149 based on daily net residual volumes and mixing volumes. While net residual volumes are state
150 variables of the hydrodynamic module of the GAMELag model, daily time series of mixing
151 volumes at frontiers of physical boxes have to be defined as forcing dataset. The
152 hydrodynamic exchanges between box 4 and physical box 1 and between box 5 and physical

box 2 only depend on mixing volume, there is no net residual volumes between these boxes. Mixing volume takes into account wind mixing (mainly inside the lagoon) and tide-driven exchange (between lagoon and the sea). These mixing volumes are therefore varying in time. A 3-dimensional hydrodynamic Model for Application at Regional Scale (MARS-3D) was used to compute daily time series of mixing volumes (Lagarde et al., 2019; Lazure and Dumas, 2008). Descriptions of the MARS3D model applied on Thau lagoon and the forcing dataset necessary for simulating water bodies circulation are provided in Fiandrino et al. (2017). Same atmospheric (wind, air temperature, incident radiation) and hydrological (daily average river water fluxes ($m^3.s^{-1}$) from the watershed) are used to force MARS-3D and GAMELag models. Specific dataset were used (sea level elevation in Sete Channel) to force MARS-3D model at the open boundary condition for the simulated period.

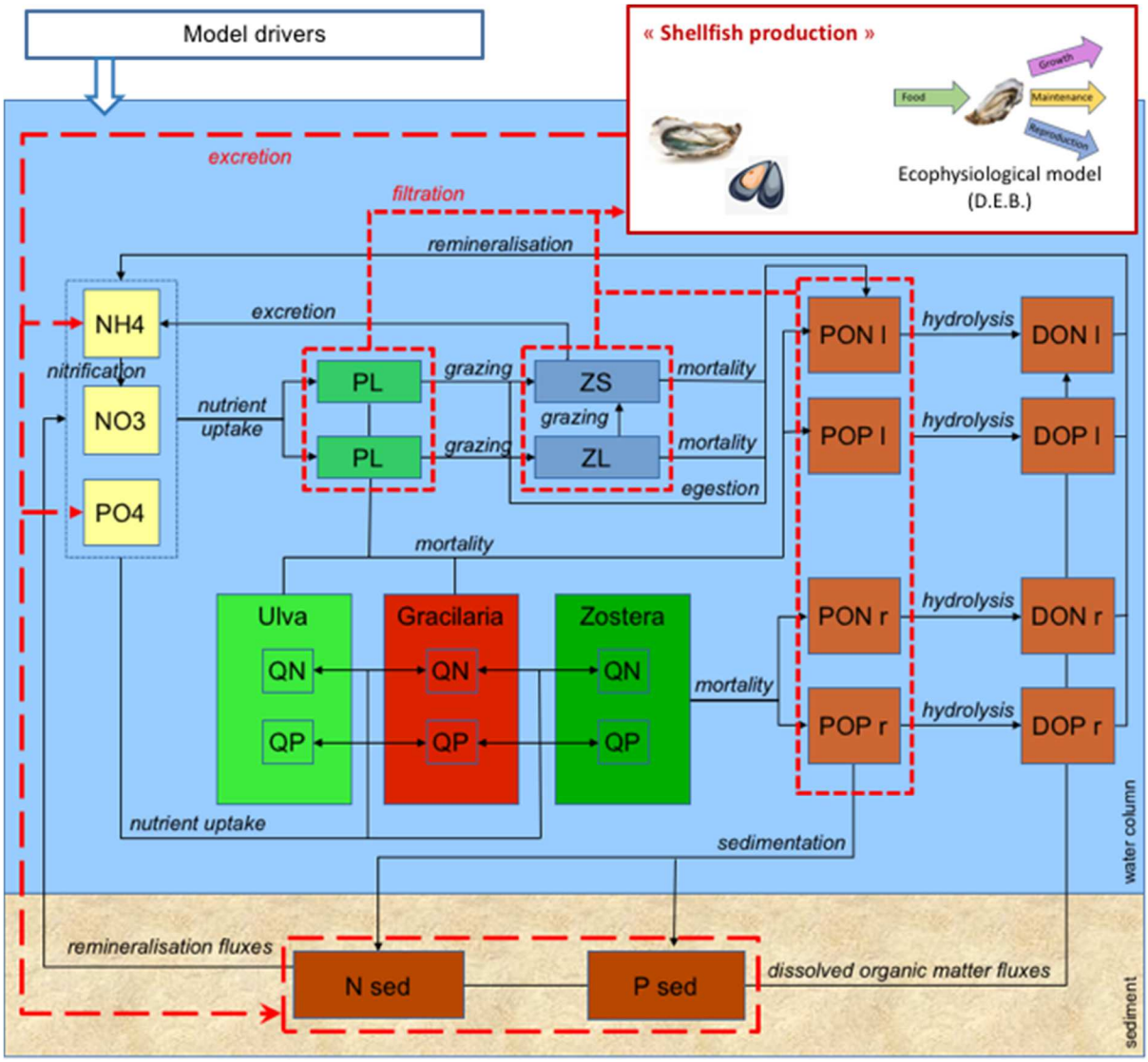

Figure 2. Conceptual scheme of the GAMELag-Conch model representing biological compartments (boxes) and processes (black arrows) within the water column (blue area) and sediment (brown area). The oyster ecophysiological model is linked to the biogeochemical cycles (red boxes) through filtration and excretion processes (red arrows).

In order to model the growth of an average oyster individual in the shellfish production areas of the Thau Lagoon, a coupling of the GAMELag and DEB oyster model was carried out to form "GAMELag-Conch" model. It involves the integration of the DEB model into the biogeochemical model. The dynamic energy budget of *C. gigas* model is based on the DEB

theory (Kooijman, 2009) and adapted to the Pacific oyster in the Atlantic under various versions, 3 state variables (Pouvreau et al., 2006) or 4 state variables (Bernard et al., 2011b). The dynamics in time of the different energy fluxes are described by a system of differential equations (see suppl. Mat. Tables S1) and associated processes (Pouvreau et al., 2006; Bernard et al., 2011b;). Within the frame of this work, the model was adapted and parameterised for the Thau lagoon with additional parameters related to rearing schemes (see suppl. Mat., Table S2).

The DEB model operates on energy flows (in joules) allocated to different functions within the individual (reserve, maintenance, growth and reproduction). Among these energy costs, some imply a dissipation of energy, which must be translated into excretion of matter to maintain steady mass balances within the GAMELag-Conch model. The oyster food resource in terms of nitrogen and phosphorus (X_N and X_P) is assumed to be a mix of various available particles in the water column (e.g. state variables of the biogeochemical model) and is defined as:

$$X_N = \alpha_{PS}PS + \alpha_{PL}PL + \alpha_{ZS}ZS + \alpha_{ZL}ZL + \alpha_{PON}PON \qquad \text{Eq. 1}$$

and

$$X_P = \frac{\alpha_{PS}PS+\alpha_{PL}PL}{NP_{phyto}} + \frac{\alpha_{ZS}ZS+\alpha_{ZL}ZL}{NP_{zoo}} + \alpha_{POP}POP \qquad \text{Eq. 2}$$

where PS, PL, ZS and ZL are small and large phytoplankton and small and large zooplankton and PON the sum of labile and refractory particulate organic nitrogen. Each of these food resources is weighted by a preference coefficient α_i with i = PS, PL, ZS, ZL, PON or POP. The oyster food resource is expressed in phosphorus using N to P stoichiometry of phytoplankton and zooplankton, (NP_{phyto} and NP_{zoo}), whereas POP is the sum of labile and refractory particulate organic phosphorus. Hence, the stoichiometry of food resources is expressed as

$$NP_X = \frac{X_N}{X_P} \qquad \text{Eq. 3}$$

The food resource and dissipated DEB energy fluxes were translated respectively from mmol N (or P) to Joules and from Joules to mmol N (or P) using conversion factors (see suppl. Mat., Table S2).

In the DEB model, some of the available energy is lost. First, there is the amount of material ingested but not assimilated by the oyster, which is expressed in the DEB model by the excretion of feces and pseudo-feces (joules per unit of time). This part of the non-assimilated food either reached the sea bed to fuel sediment stock of N and P or was remineralised into inorganic nitrogen and phosphorus in the water column. Once assimilated, the energy is allocated into the compartments of the DEB model (structures, reserves and reproduction). In order to maintain balanced stoichiometry in the DEB model, excretion is required and is simulated according to the stoichiometry of the ingested material. Thus, the ratio N: P of the resource (NP_X) is compared to the ratio N:P of the oyster (NP_O). When this NP_X is greater than the NP_O, the regeneration of material is in the form of ammonium in the model. On the contrary, when the NP_X is lower than the NP_O, the regeneration was assumed to be in the form of orthophosphate. In this way, even if the stoichiometry of the resource is variable, the individual rejects a quantity of N or P to maintain a balanced stoichiometry. This system of regeneration of post-assimilation material provides available mineral forms of N and P in the water column. The maintenance costs ($\dot{p}_M + \dot{p}_J$) (Eq. 4), growth costs ($\dot{p}_G\ (E_G - d_V \times \mu_V) / E_G$) (Eq. 5) and gamete production costs ($\dot{p}_G\ (E_{GGo} - d_{Go} \times \mu_{Go}) / E_{GGo}$) (Eq. 6) were also added to the amounts of regenerated matter as they correspond to dissipated energy (see suppl. Mat., Table S3). In the GAMELag-Conch model, these energy costs were converted into NH_4^+ or PO_4^{3-} with conversion factors C_{oyster} and μ_{EN} (energy yield of reserves). These conversion factors are based on the available data on the chemical potential of the different compartments of the oyster (Add-my-pet portal: https://www.bio.vu.nl/thb/deb/deblab/add_my_pet/). Thus, the chemical potential of the food,

once converted to J $mmol^{-1}$ N, gives a conversion factor, C_{oyster}, of 3250 J $mmol^{-1}$ N. The C_{oyster} conversion factor affects energy related to ingested but non-assimilated matter (feces and pseudo-feces) and the energy related to predation on the different compartments composing oyster food (ie, small and large phytoplankton, small and large zooplankton and particulate organic matter). The second conversion factor, μ_{EN}, is obtained by deriving the chemical potential of bivalve reserves with the nitrogen (or phosphorus) content of the organic matter that makes up these reserves. The factor thus obtained is 3667 J $mmol^{-1}$ N. In general, these conversion factors vary between 2400 and 3700 J $mmol^{-1}$ N depending on whether food, structure or reserves are considered as N or P content (Platt and Irwin, 1973; Grangeré et al., 2009).

2.3 Oyster seeding scheme in the model

Seeding scheme, as the introduction in farming structures of spats and oysters, is rather complex in the Thau lagoon and mainly depends on environmental conditions, contamination risks time frame or market dynamics. Two main periods for seeding were extracted from the monograph results (Cepralmar, 2016) indicating that, according to growth durations, most spats (6 to 8 mm) were mainly reared on lanterns or pearl nets and introduced between July and August (47% reared over the summer) for a period of 6 to 8 months. In addition, this study indicated that oysters (15 to 20 mm) were introduced within the early months of the year (53% in January and February) for a duration of 12 to 14 months to reach marketable-size oyster. Therefore, in order to simplify this seeding time schedule for the GAMELag-Conch model, we assumed a common seeding scheme where oysters were introduced on the first of February and harvested in mid-December. Regarding to spat seeding, the first of July was used in the model to start growth of spats for a duration of 7 months. In February, remaining spats from year n were then used to seed oysters in year n+1. The total abundances

250 were 532.1 10^6 and 235.7 10^6 individuals for spats and oysters respectively for the entire
251 farming zone (box 4 + box 5, Figure 1). Mortality rates were also extracted from the
252 monograph with values of 38.2% (10.5 x10^{-4} d^{-1}) during the pre-growing phase and 32.5%
253 (8.9 10^{-4} d^{-1}) during the growing phase (Cepralmar, 2016). Seeding densities were then used
254 to simulate stocking densities over the growing period as follows:

255 $$\frac{dOyster}{dt} = Seeding_{Oyster} - Oyster \times mortality_{Oyster}$$ Eq. 7

256 And

257 $$\frac{dSpat}{dt} = Seeding_{Spat} - Spat \times mortality_{Spat}$$ Eq. 8

258 Where $Seeding_{Oyster}$ and $Seeding_{Spat}$ are densities of oysters and spats introduced as
259 described above. The number of individuals introduced was extracted from the monograph
260 (Cepralmar, 2016) and extrapolated to the farming zones with data from local authorities
261 (DDTM, 2014), which represented an average exploitation of 70% of growing structures.
262 Length (L) and dry flesh matter (DFM) were calculated at harvest for each simulated year.
263 Annual oyster production was estimated from total weight (derived from DFM, equation 16,
264 Table S1 in suppl. Material) and the number of living individuals simulated at harvest. Oyster
265 condition index (CI, %) was estimated from model outputs by using the ratio of DFM (g) over
266 Length (cm).
267
268 2.4 Reference simulation
269 The baseline simulation (e.g. “Reference”, scenario n°1, Table 1) used in this study
270 represented the current conditions of the Thau lagoon functioning. This baseline simulation
271 was used to evaluate model skills (see section 2.5). This simulation covered the period from
272 2014 to 2016 and was carried out with the hydro-meteorological conditions of these three
273 years including precipitation, contributions of the natural catchment and contributions from

WWTP, based on the data of self-monitoring recorded at the entrance of the WWTP (data from SMBT).

Table 1. Summary of scenarios tested with reference simulation, watershed nutrient inputs and shellfish densities described according to their characteristics.

Type of scenario	*Scenario number*	*Characteristic*	*Observation – management interest*	*Name of scenario in figures*
Reference	1	Current stocking densities, WWTP outputs estimated from current average abatements	Use as a standard for comparing scenarios	Ref
Watershed inputs	2	Maximum yield on N& P for all WWTP (≥ 90% on both N & P)	Correspond to the scheme for water management (SAGE)	Max. yield
	3	Normal yield on N & P for all WWTP (75% N, 60% P)	Classification off « sensitive zone » to eutrophication	Nal yield
	4	Projection of an increase in the number of inhabitants in the territory	Correspond to the comprehensive territorial occupation scheme (SCOT) predicting a 23% increase of the population in the Thau watershed by 2030	SCOT
	5	Partial release of water and nutrients from the Sète WWTP into the lagoon	Operating strategy of Sète WWTP	Sète
Shellfish farming	6	Seeding to the maximum of the growing structure capacity according to the « structure scheme (DDTM)	Evaluation of the effect of the maximum capacity of breeding structures on the lagoon ecosystem and oyster production and performances	Max. dens.

Hydrological conditions of the simulated years were contrasted in terms of total rainfall and associated trophic contributions. The year 2015, defined as a dry year (-255 mm compared to 1970-2016 average), showed low natural hydrological contributions with inputs of 0.77 t of P and 12.7 t of N, whereas the years 2014 and 2016, with more intense rainfall events (+70 mm and -55 mm compared to 1970-2016 average), brought natural nutrient loadings to a respective estimate of 5 and 5.6 t of P and 86.6 t and 98 t of N. During wet years, anthropogenic inputs from WWTP amounted for 18% of N loading against 55% for P inputs. Total inputs from the watershed (natural and anthropogenic) reached 109.2, 39.4 and 113.8 tons of N and 10.1, 6.1 and 10.2 t of P for the three simulated years. For the year 2015, WWTP discharges constituted the main source of N (62%) and P (90%) inputs, whereas for

289 the wet years 2014 and 2016, WWTP inputs accounted for up to 20% of total nutrient
290 loadings. The initialization of the biological compartments takes into account the most recent
291 observations in order to get as close as possible to the current conditions in the simulations.
292 Concerning the initialization of shellfish culture, data from the Cépralmar monograph
293 (Cépralmar, 2016) were used for livestock densities in the Bouzigues and Mèze-Marseillan
294 areas (see section Oyster seeding scheme in the model). The extrapolation of these survey
295 results to both production areas was based on the data provided by local authorities (DDTM,
296 2014) with 2632 tables in concession of which 382 were not active. The estimate of the
297 structures hosting pre-growth (spats) and growth (adults) was conducted using data from the
298 monograph (Cepralmar 2016) extrapolated to the 2250 tables in operation on each of the two
299 areas. This baseline scenario is referred as "Ref" in table 1 (scenario n°1, Table 1).
300
301 2.5 Model skills evaluation & model computation
302 The Willmott index of agreement (Willmott, 1981), d, was used to evaluate the performance.
303 This metric is a standardized measure of the degree of model prediction error and varies
304 between 0 and 1. A value of 1 indicates a perfect match, and 0 indicates no agreement at all.
305 This index of agreement was used to evaluate model skills on salinity, Chl *a* concentration as
306 well as shell length (cm) and tissue dry weight (g) of cultured oysters. Available observations
307 for these variables were compared to simulations for the two shellfish farming zones (Figure
308 1, box 4 and 5). The GAMELag-Conch model was implemented in R (R Core Team, 2017),
309 using the deSolve package (Soetaert et al., 2010) for differential equation solving (time step: 1
310 day).
311
312 2.6 Description of scenarios

313 Scenarios of different nutrient inputs and shellfish culture strategies were determined in close
314 interactions with shellfish farmers (Mediterranean shellfish committee, CRCM), managers
315 (the Thau basin organization, SMBT; the Centre for studies of lagoon and maritime activities,
316 CEPRALMAR; the French water agency, AERM&C; Departmental Direction of Territories
317 and Sea DDTM) and scientists (MARBEC). These scenarios were built on realistic
318 management hypotheses, established during participative meetings and are based on two main
319 axes: 1) scenarios related to trophic contributions from the watershed and associated
320 management measures and 2) scenarios related to shellfish production and they are
321 summarized in Table 1.
322 The anthropogenic contributions of the watershed were tested according to different scenarios
323 corresponding to different management hypotheses around the watershed of Thau (Scenario 2
324 to 5, Table 1). The yields of the WWTPs are constrained by the environment that receives the
325 discharges and come within the context of the Regional Plan for Water Management (SDAGE
326 Rhône-Méditerranée) and the local Water Management Scheme (SAGE) applied to the Thau
327 lagoon territory. When these receiving water bodies carry a risk of eutrophication, they are
328 classified as sensitive to eutrophication according to European regulation (EC, 1991). In the
329 context of "sensitive zones", the European legislation (EC, 1991) requires WWTP to treat at
330 least 80% of phosphorus and 70 to 80% of nitrogen for cities with more than 10 000
331 inhabitant equivalents (IE). For smaller municipalities, these obligations vary and may be
332 higher depending on the case. Thau lagoon was classified as a “sensitive zone” in 2004
333 according to European recommendations (EC, 2004). On these provisions, it was concluded
334 to test initially two scenarios declining these treatments of WWTP to: 1) maximum yield
335 (scenario 2: Max. yield) with abatements greater than 90% for nitrogen and phosphorus; 2)
336 normal yield (scenario 3: Nal yield) corresponding to reductions of 75% and 60% respectively
337 for nitrogen and phosphorus. It should be noted that only the Mèze lagoon-based treatment

338 plant currently offers yields comparable to the high abatements required by the "sensitive
339 zone" classification (> 90%).
340 In direct relation with the environmental management constraints, the territorial occupation
341 scheme (SCOT) and, in particular, the demographic projections of this SCOT, were evaluated
342 in this study. Indeed, an increase in population (estimated at 23% at 2030 horizon) directly
343 leads to increased WWTP effluents (wastewater discharges) and, consequently,
344 recommendations to anticipate these evolutions must be incorporated into a management
345 policy of the territory. This scenario (Scenario 4, “SCOT” Table 1) aimed at estimating the
346 impact of the population increase on the Thau catchment area by 2030 in terms of nitrogen
347 and phosphorus inputs to the lagoon, as well as its impact on ecological status and shellfish
348 cultures in the Thau lagoon. Current yields of WWTPs were then applied to these estimated
349 quantities of nitrogen and phosphorus to provide quantities entering the lagoon.
350 The following scenario (scenario 5; “Sète”, Table 1) corresponded to potential management
351 leverage for freshwater and nutrient inputs (N & P) to the lagoon through an operating
352 strategy of the Sète WWTP. This scenario addressed the question of the evaluation of the
353 impact of discharges in the Sète channels and hence in the lagoon, in anticipation of important
354 modernization works on the WWTP. The Sète WWTP currently has its outfall in the sea but
355 could release discharges to the Sète channels in case of heavy rains. This scenario examined
356 the effect of an additional 69.5, 72.9 and 84.7 tons of nitrogen in 2014, 2015 and 2016
357 respectively. In terms of phosphorus, additional quantities were estimated at 3.7, 3.1 and 3.6
358 tons for the same years respectively.
359 The scenario of different oyster stocking densities tested in this study corresponded to seeding
360 conditions for which all the growing structures would be filled with oysters at the maximum
361 densities allowed by the structure scheme (DDTM, 2014). In comparison to reference seeding
362 conditions (see section Oyster seeding scheme in the model), abundances were increased by a

363 factor 2 for spats (e.g. 501 10^6 and 546 10^6 individuals for box 4 (Bouzigues) and box 5
364 (Mèze-Marseillan), respectively) and by a factor 1.3 for oysters (e.g. 158.7 10^6 and 129.9 10^6
365 individuals for box 4 and box 5, respectively).
366
367 2.7 Data treatment and scenario realization
368 Prior to the simulations of these different scenarios, a first step was the WWTP data
369 processing to force the GAMELag-Conch model. Work to recover volumes and
370 concentrations of global nitrogen (NGL) and global phosphorus (PGL) at the inlets of the
371 WWTPs was performed based on data from SANDRE (portal:
372 http://www.sandre.eaufrance.fr). These data were used to establish: 1) yield matrices, for each
373 WWTP located on the Thau watershed, and 2) matrices of fractions of the different forms of
374 nitrogen and phosphorus for each of the WWTP, to allow the transformation of total nitrogen
375 and total phosphorus after treatment into their different inorganic and organic fractions
376 necessary to force the model.
377 In a first step, the input data of WWTP undergoes a reduction corresponding to the scenario
378 tested (see abatements, Table 1) and in a second step, the output concentrations thus estimated
379 are fractionated according to the different forms of nitrogen and phosphorus for the
380 corresponding WWTP. This procedure allowed for multiple different yield matrices (or input
381 augmentations as per SCOT projections) applied to the same starting NGL and PGL datasets.
382 This method was applied for all scenarios with three matrices of yields covering current
383 treatment, maximum treatment and normal treatment (see sections on Reference and scenarios
384 description).
385
386 2.8 Carrying capacity evaluation

As mentioned in the introduction, the targeted carrying capacity lies in the equilibrium between an optimised harvest without negative effects on ecological functioning. The dame index and phytoplankton depletion index were then used where the former provides a bulk information on ecosystem functioning and allows comparison between different ecosystems. Whereas the depletion index linked more finely cultured bivalves to its resource.

2.8.1 Dame index

The Dame index was calculated from the characteristic times of the lagoon (Dame and Prins., 1998). These characteristic times included: i) the lagoon renewal time (RT: time required to renew the entire lagoon volume) which is a hydrodynamic feature, ii) the phytoplankton renewal time (PPT: equivalent to the ratio of the average phytoplankton biomass to average gross primary production); and finally, iii) the clearance time (CT: time required for the total stock of shellfish to filter the lagoon volume).

The renewal time (RT) was calculated for the whole lagoon using the volumes entering the lagoon by the Sète channel:

$$RT = \frac{V_{lagune}}{\overline{V_{in}}} \qquad \text{Eq. 9}$$

Where V_{lagune} and $\overline{V_{in}}$ were the volumes of the lagoon (m^3) and mean annual incoming volume ($m^3\ d^{-1}$), respectively. This formulation gave renewal times of 48.6, 48.4 and 48.8 days for the years 2014, 2015 and 2016 respectively. These RT values were in agreement with the field observations reported by Fiandrino et al. (2012) where RT ~ 50 days.

The phytoplankton renewal time (PPT) was obtained by the ratio of the annual mean phytoplankton biomass (estimated from the Chl *a* concentration expressed in mmol N m^{-3}) on the mean daily gross primary production (estimated from the phytoplankton growth calculated by the model and expressed in mmol N $m^{-3}\ d^{-1}$).

410 The clearance time (CT), time required for cultured oysters to filter the volume of the lagoon,
411 was calculated taking into account the oyster filtration rate according to the formulation of
412 Bougrier et al. (1995):

413 $$Filtration\ rate = 4{,}825 - (0{,}013 \times (T_{\circ C} - 18{,}954)^2) \times DFM^{0{,}439} \quad \text{Eq. 10}$$

414 Where $T_{\circ C}$ was the temperature in degrees Celsius and DFM the dry weight (g) at harvest.
415 The filtration rate was expressed in L ind^{-1} h^{-1}. The clearance time CT was expressed by
416 comparing the filtered volume with the average volume of the lagoon:

417 $$Clearance\ time = \frac{Vol_{lagoon}}{filtration\ rate \times nb\ of\ individuals \times {}^{24}/_{1000}} \quad \text{Eq. 11}$$

418 where the filtration rate was extrapolated to the number of cultured individuals for a day and
419 expressed in m^3 d^{-1} and Vol_{lagoon} (m^3) to give a clearance time in days.
420 All these characteristic times were expressed in days and their ratios (CT:RT and CT:PPT)
421 potentially inform on the capacity of the lagoon to support or not a sustainable shellfish
422 production. The CT:RT ratio indicated whether filter feeders and its resources were controlled
423 by exchanges with the sea or by internal (including inputs from the watershed) availability of
424 nutrients. The CT:PPT ratio expressed directly the link between the resource and the shellfish
425 culture, where a ratio of 1 would indicate that all phytoplankton primary production was
426 consumed by filter feeders in culture and would therefore be a critical value.
427 *2.8.2 Lagoon-scale phytoplankton depletion index*
428 At the scale of the lagoon area, a phytoplankton depletion index (Filgueira et al., 2014a) was
429 calculated to determine the impact of shellfish farming on its main resource. This index
430 compared the average phytoplankton biomass in farming areas (box 4 and 5, Figure 1) with
431 the phytoplankton biomass produced outside these zones (off-table: boxes 1, 2 and 3; Figure
432 1). Negative values indicated a depletion in nutritive resource, whereas positive values
433 indicated sufficient resource for the growth of bivalves.

$$Lagoon - scale\ depletion\ index = \frac{\overline{[Chla]}_{farms}}{\overline{[Chla]}_{off-table}} \times 100 - 100 \quad \text{Eq. 12}$$

This formula compared the daily average Chl *a* concentration of all shellfish growing areas (box 4 and 5, Figure 1) with the daily average Chl *a* concentration for all off-table areas (boxes 1, 2 and 3, Figure 1).

This index may be gauged against the natural variability of the phytoplankton biomass to evaluate the sustainability of the shellfish farming activity (Grant and Filgueira, 2011). This lagoon-scale depletion index is asymmetrical and a value of -100% indicates a complete depletion, whereas enrichment has no upper limit. For this reason, the median annual values of this index were preferred to mean values and were used to compare the scenarios.

2.9 Ecological indicators and ecological status

The compartments of the model relative to the dissolved organic and inorganic matter were used to estimate summer nutrient concentrations. 90th percentiles (p90) were calculated from the 92 daily values obtained from June 1st to August 31st for each simulated year, of dissolved inorganic nitrogen (DIN= NO_3^- + NH_4^+), dissolved inorganic phosphorus (DIP), total nitrogen (TN: dissolved and particulate inorganic and organic nitrogen as well as the two "small" and "large" phytoplankton compartments) and total phosphorus (TP: inorganic phosphorus and dissolved and particulate organic and phytoplankton compartments expressed as phosphorus using the Redfield (1963) N:P ratio of 16). These four variables DIN, DIP, TN and TP, represented estimates of the WFD indicators measured for the diagnosis of the ecological status of lagoon water bodies (Derolez et al., 2013). These simulated indicators were used to compare the “Reference” scenario with actual observations and the influence of the different scenarios tested on the ecological status. The model also estimated Chlorophyll *a* concentration in the water column using the "small" and "large" phytoplankton variables. These two state variables were expressed in mmol N m^{-3} in the model and converted to µg

459 Chl *a* l^{-1} using a conversion factor of 1 (Parsons et al., 1961). The summer averages obtained
460 from the simulations were used as an indicator of the phytoplankton biomass as in the WFD
461 diagnosis. Finally, the TN to TP ratio was used as an indicator of nitrogen and phosphorus
462 balance within the system.
463
464 2.10 Statistical analyses
465 Data did not fulfilled tests for both normality and homosedasticity and non-parametric,
466 Kruskal-Wallis, was therefore used for statistical analysis. Correlations were determined
467 following Spearmann correlation coefficient, ρ. Statistical analyses were considered
468 significant with p-value < 0.01. Principal component analysis (PCA) was performed on model
469 outputs presented in this work. All statistical analyses were performed using the R software
470 (R Core Team, 2017).
471
472 3 Results
473 3.1 Model skills
474 Model skills evaluation was based on model outputs of the "Reference" scenario representing
475 current situation. The GAMELag-Conch model satisfactorily simulated observations of
476 salinity (Figure 3-A) for both shellfish farming zones with a Willmott index "d" of 0.96
477 (linear regression $r^2 = 0.91$). This agreement between observed and simulated values
478 prevailed the good representation of the lagoon hydrodynamics when described by 3 physical
479 boxes (see "Carrying capacity model" description").
480 Similar to salinity, model outputs were correctly correlated with the observed length (Figure
481 3-C) and dry weight (Figure 3-D) of oysters, with Willmott index of 0.69 ($r^2 = 0.77$) and 0.76
482 ($r^2 = 0.76$) respectively.
483

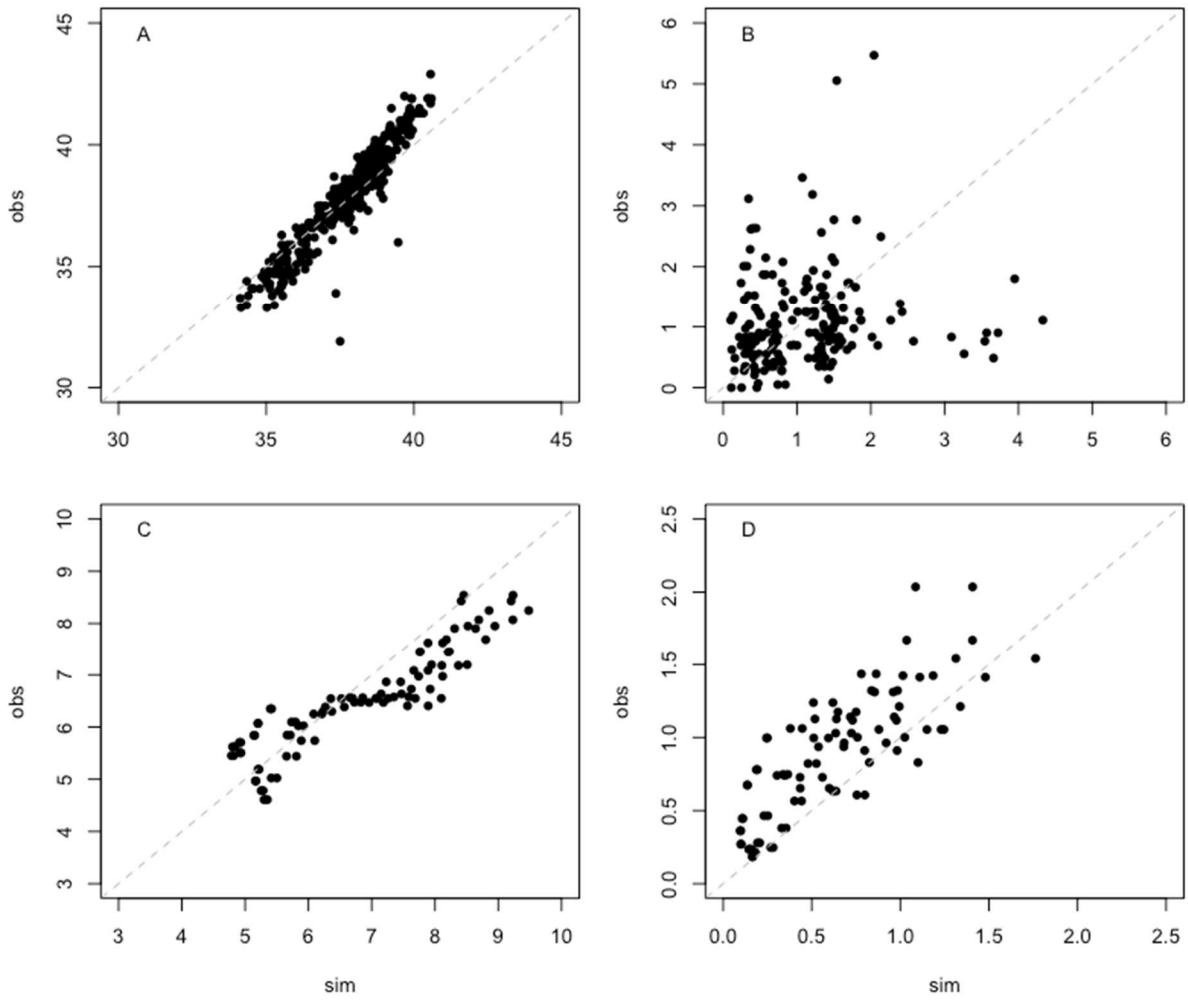

Figure 3. Biplots of simulated vs. observed salinity (A), Chl *a* concentration (µg l^{-1}, B), oysters shell length L (cm, C) and oyster dry weight (g, D) extracted from model outputs within the two shellfish farming zones (box 4 and 5).

A poorer Willmott index was found for the Chl *a* variable at d=0.46 (r^2 = 0.03). The comparison of observations against simulations indicated that simulated Chl *a* concentrations were within the range of observations for concentrations lower than 2.5 µg Chl *a*.L^{-1}. However, the model could not capture the timing of extreme values (peaks), which explained the mismatch on Figure 3-B for high Chl *a* concentrations.

3.2 Nutrients inputs and shellfish performances

For the three simulated years and all the scenarios, annual nutrient inputs varied from 25.5 to 198.6 tons of nitrogen and from 1.8 to 13.8 tons of phosphorus (Table 2). These ranges included lower and higher values of nutrient inputs than that of the Reference scenario (39.4 to 111.5 t of N and 6.1 to 10.2 t of P, Table 2). Results presented in Fig. 4 and Table 2 highlighted the significant variability of oyster performances (weight and production) according to years and scenarios of nutrient inputs. The variability of oyster production as well as total weight of oyster, was mainly controlled by the hydrometeorology, with oyster production being 1.8-2.3 times higher during rainy years than dry years whatever the tested scenario (Table 2). Total weight of oysters at harvest varied between 36.6 to 100.5 g (Table 2) according to scenarios and simulated years. Similar to production, total weight was significantly higher in wet years than dry years (Kruskal-Wallis, $p < 0.05$), although no significant differences were found between scenarios. In comparison to the current situation (Reference), higher oyster productions were simulated with normal waste water treatment plant efficiency (Normal Yield: □75% N, □60% P) with an additional 1700 t produced during dry years corresponding to an increase in production of 25%. This increase was less important during wet years (940-1200 t, +5-7%). By contrast, maximum WWTP efficiency (Max yield □90% N & P) induced a mean decrease of 1598 t, corresponding to a decrease of 12% in comparison with mean reference production. The foreseen increase in population (SCOT scenario) induced a mean increase in oyster production of 5%. Finally, in the Séte scenario, oyster production was not enhanced and recorded 875 t less than reference production (Table 2), while nitrogen and phosphorus inputs were significantly higher than reference (1.8-2.8 times more N and 1.3-1.5 more P). Scenario of oyster stocking density to its authorized maximum (by the French regulation body) triggered a mean increase of oyster productions by 7% at the expenses of thinner oysters with a lower condition index.

Table 2. Summary of simulations inputs and outputs for the three years (2014-2015-2016) and the six scenarios tested.

	Annual N inputs (t)	Annual P inputs (t)	Inputs N:P molar ratio	Production at harvest (tons)	Length at harvest (cm)	Total weight at harvest (g)	Condition index at harvest (%)	Ecological status [a] [NID-PID-TN-TP-CHLA-TN:TP] Summer – P90 – (µM)	RT (days)	CT (days)	PPT (days)	Median lagoon-scale depletion index (%)
Reference												
2014	109.2	10.1	23.9	16977	9.5	93.7	17.5	[0.31-0.50-16.00-1.29-1.68-13.52]	48.6	17.4	6.3	-14.1
2015	39.4	6.1	14.3	7896	8.0	43.6	9.7	[0.49-0.45-20.35-1.39-3.57-18.52]	48.4	20.1	7.1	-12.8
2016	113.8	10.2	24.7	12208	8.8	67.4	13.6	[0.34-0.46-18.56-1.35-3.43-16.65]	48.8	18.2	7.4	-14.0
Mean ± sd	87.5 ± 41.7	8.8 ± 2.3	21.0 ± 5.8	12360 ± 4542	8.8 ± 0.8	68.2 ± 25.1	13.6 ± 3.9	[0.38-0.47-18.30-1.34-2.89-16.23]	48.6 ± 0.2	18.6 ± 1.4	6.9. ± 0.6	-13.6 ± 0.7
Max. yield												
2014	93.9	5.8	35.7	15606	9.4	86.2	16.3	[0.31-0.41-15.64-1.19-1.70-14.56]	48.6	17.3	6.0	-14.2
2015	25.5	2.0	28.8	6669	7.5	36.8	8.7	[0.50-0.48-21.15-1.48-3.90-18.88]	48.4	19.8	7.2	-12.4
2016	100.2	6.3	35.5	10011	8.3	55.2	11.8	[0.34-0.47-19.18-1.40-3.62-17.82]	48.8	18.0	7.4	-13.7
Mean ± sd	73.2 ± 41.4	4.7 ± 2.4	33.3 ± 3.9	10762 ± 4515	8.4 ± 0.9	59.4 ± 25.0	12.3 ± 3.8	[0.38-0.46-18.65-1.35-3.07-17.09]	48.6 ± 0.2	18.4. ± 1.3	6.9 ± 0.7	-13.4 ± 0.9
Normal yield												
2014	118.6	12.3	21.4	18194	9.6	100.5	18.7	[0.31-0.54-16.27-1.35-1.68-13.19]	48.6	17.4	6.6	-14.0
2015	46.4	8.1	12.7	9838	8.4	54.3	11.6	[0.49-0.40-19.43-1.30-3.14-18.59]	48.4	20.6	7.1	-13.3
2016	20.8	12.2	22.0	13909	9.2	76.8	14.9	[0.32-0.42-17.73-1.27-3.15-16.65]	48.8	18.4	7.5	-14.2
Mean ± sd	95.3 ± 42.3	10.8 ± 2.4	18.7 ± 5.2	13981 ± 4178	9.0 ± 0.6	77.2 ± 23.0	15.0 ± 3.6	[0.37-0.45-17.81-1.30-2.66-16.14]	48.6 ± 0.2	18.8. ± 1.7	7.1 ± 0.5	-13.8 ± 0.5
SCOT												
2014	114.8	11.2	22.6	17894	9.6	98.8	18.4	[0.31-0.52-16.14-1.32-1.67-13.32]	48.6	17.4	6.4	-14.0
2015	44.6	7.2	13.7	8610	8.2	47.5	10.3	[0.50-0.43-19.97-1.35-3.41-18.58]	48.4	20.3	7.1	-13.0
2016	118.9	12.2	23.3	12571	9.0	69.4	13.8	[0.33-0.45-18.35-1.32-3.27-16.61]	48.8	18.3	7.4	-14.2
Mean ± sd	92.8 ± 41.7	9.9 ± 2.3	19.9 ± 5.4	13025 ± 4658	8.9 ± 0.7	71.9 ± 25.7	14.2 ± 4.0	[0.38-0.47-18.15-1.33-2.79-16.17]	48.6 ± 0.2	18.7. ± 1.5	7.0 ± 0.5	-13.7 ± 0.6
Sète												
2014	178.7	13.8	28.7	16616	9.5	91.8	17.1	[0.31-0.48-16.84-1.30-1.68-14.13]	48.7	17.3	5.9	-14.2
2015	112.3	9.2	26.9	7184	7.8	39.7	9.1	[0.51-0.50-22.35-1.52-3.91-18.92]	48.5	20.0	6.8	-12.6
2016	198.6	13.6	31.7	10654	8.5	58.8	12.4	[0.34-0.50-20.71-1.47-3.68-18.14]	48.9	18.0	7.2	-13.8
Mean ± sd	163.2 ± 45.2	12.3 ± 2.6	29.1 ± 2.4	11485 ± 4770	8.6 ± 0.9	63.4 ± 26.4	12.9 ± 4.0	[0.39-0.49-19.97-1.43-3.09-17.06]	48.7 ± 0.2	18.5 ± 1.3	6.6 ± 0.6	-13.6 ± 0.8
Max density												
2014	109.2	10.1	23.9	18735	9.3	85.8	16.5	[0.31-0.52-16.00-1.31-1.87-13.46]	48.6	14.1	6.0	-15.1
2015	39.4	6.1	14.3	7976	7.8	36.6	8.3	[0.44-0.48-20.57-1.44-3.69-18.41]	48.4	16.1	6.8	-13.4
2016	113.8	10.2	24.7	12936	8.5	59.2	12.5	[0.34-0.54-19.16-1.47-3.56-16.57]	48.8	14.8	7.1	-14.5
Mean ± sd	87.5 ± 41.7	8.8 ± 2.3	21.0 ± 5.8	13216 ± 5385	8.5 ± 0.7	60.6 ± 24.7	12.4 ± 4.1	[0.38-0.43-17.00-1.24-2.35-16.07]	48.6 ± 0.2	15.0 ± 1.0	6.7 ± 0.6	-14.3 ± 0.9

[a]: ecological status based on 90th percentile on indicators: NID, PID, TN, TP and Chla. Color code gives the class of these indicators: "High" (blue), "Good" (green), "Average" (yellow), "Bad" (orange) and "very bad" (red).

To conclude oyster production, the comparison of scenarios showed that only “Sète” (n°5) and “Max. yield” (n°2) scenarios induced lower oyster production than “Reference” scenario exhibiting a decrease of 8 and 16 % respectively. All other scenarios that involved increased nutrient inputs, “Nal yield” (n°3) and “SCOT” (n°4), presented higher oyster production levels with sensibly higher shell length and total weight (Table 2). On the contrary, if scenario “Max. dens.” (n° 6) rendered higher oyster production than “Reference” scenario, no increase of length or total weight of individuals was apparent. Oyster condition index (CI) was used as a proxy for the health of oysters and was significantly lower in 2015 (Kruskal-Wallis, $p < 0.05$) with no differences between scenarios.

When discriminating dry and wet years, according to the different nitrogen and phosphorus inputs simulated, one can note on Figure 4 that oyster production values were maximized for a mass ratio N:P of the watershed contributions around 8.3 (that is, about 100 t N for 12 t P or a molar ratio of 18.4; Figure 4).

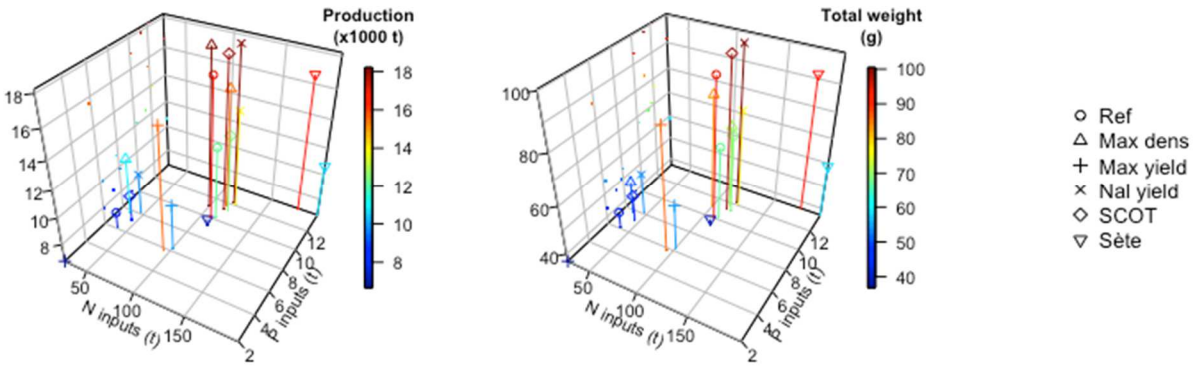

Figure 4. 3D scatter plot of production (10^3 t) and total weight (g) of oysters as function of N and P inputs (t) according to scenarios and years (see legend inset).

This seemingly optimal N:P ratio was obtained for the scenarios varying nutrient loadings "Nal yield" (n°3), "SCOT" (n°4) and “Reference” during" wet years (2014 & 2016) but not during 2015 (Table 2) where N:P ratio was 6.6.

In fact, the nitrogen inputs according to the different scenarios during the dry year (2015) varied from 25% to 50% of those during the two wet years (2014 and 2016) with the largest difference between dry and wet years recorded for the "Max. yield" scenario (Table 2). For phosphorus, the variability of the contributions according to the hydrometeorology was less marked. Nevertheless, inputs of phosphorus in the dry year were 1.5 to 3 times lower than for wet years. This difference between wet and dry years was also largely marked by a significant modification of the contribution of the WWTP to the total inputs of the watershed reaching 89% on average in a dry year. Nitrogen to phosphorus mass ratios of inputs varied from 4.6 to 16.0 (10-35 mol:mol) depending on the year and scenario and encompassed the optimal 8.3 N:P value linked to the highest oyster productions obtained in our simulations.

3.3 Carrying capacity

While renewal time (RT) seemed constant and corresponded to 48.6 days (Table 2), phytoplankton biomass renewal time (PPT) and clearance time (CT) varied according to scenarios with minimal and maximal means observed for "Max density" and "Normal yield" scenarios respectively (Table 2). The CT:RT ratio remained constant regardless of the nutrient loading scenario (mean of 0.38) and was lower as part of the "Max density" scenario (mean 0.30), indicating that water renewal times exceeded clearance times. The CT:PPT ratios ranged from 2.06 to 2.93 with minimal mean observed at "Max density" (Table 2, Figure 5), indicating that shellfish culture pressure on phytoplankton was not critical, because clearance time was of 34% to 50% of phytoplankton production potential. In other words, the renewal time of phytoplankton production in the Thau lagoon was systematically twice as fast as the time required for oysters to filter all the phytoplankton biomass produced. This "Max. density" scenario led to the lowest CT:PPT ratios with values of 2.13, 2.45 and 1.98 for 2014,

2015 and 2016 respectively, revealing a stronger pressure of shellfish farming on its phytoplankton resources than the other scenarios.

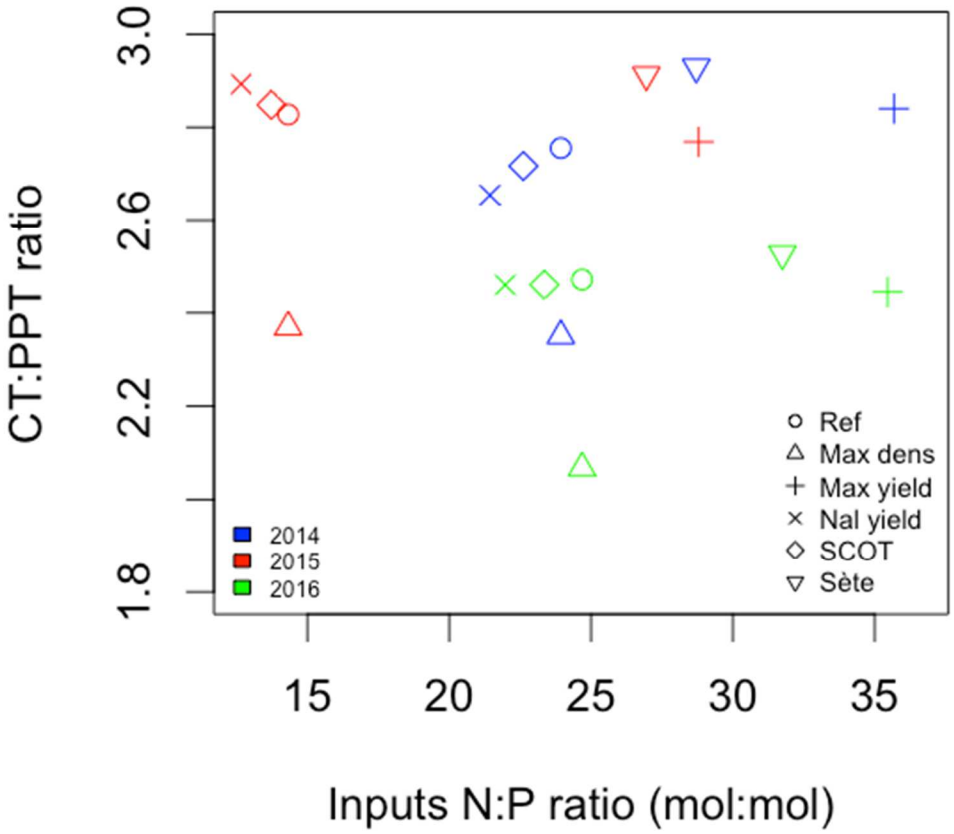

Figure 5. Clearance time to phytoplankton renewal time ratio as a function of inputs N:P molar ratios plotted for the 3 simulated years and all scenarios (see legend inset).

This pressure was accompanied by the lowest lagoon-scale phytoplankton depletion index over these three simulated years (Table 2). The CT:RT and CT:PPT ratios showed no significant correlation with N:P ratio of catchment inputs.

For the "Reference" scenario presented (Figure 6), the median value of this index varied between -14% and -13% indicating that the lagoon was in slight depletion conditions but may support shellfish production. The median lagoon-scale depletion indices appeared consistently negative, regardless of the scenario tested (Figure 6-A, B & C). Overall median lagoon-scale

depletion indices varied between -12.3 and -15.1% depending on the year and scenarios tested, but they did not show a clear trend depending on the amount of nitrogen or phosphorus brought by the watershed (Figure 6- A and B). The range of values of the median depletion index was bounded by the scenarios "Max. density" and "Max. yield". The difference between simulated years was the main contrast between these median values of the depletion index (Kruskal-Wallis, p-value <0.01). Figure 6-C showed these median depletion indices as a function of the N:P ratios of the catchment contributions and the values of these indices decreased with decreasing N:P ratio of watershed inputs in 2015 and 2016 (Spearman correlation coefficient of -0.83 and -0.94, respectively).

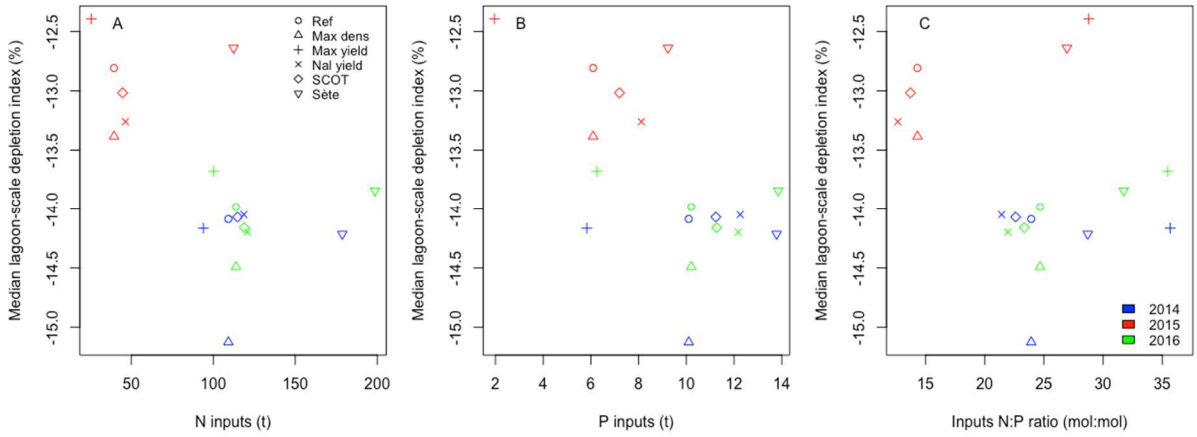

Figure 6. Median lagoon-scale depletion index expressed as a function of N inputs (A), P inputs (B) and inputs N:P molar ratio (C).

3.4 Ecological Status

Although carrying capacity can be assessed through different indices, ecological status of the lagoon must be regarded as another major characteristic depending on nutrient loadings or shellfish culture practices. The p90 summer concentrations of DIN, DIP, TN and TP, derived from the "Reference" simulations (Figure 7-A, B & C) were consistent with the concentrations observed in the water column of Thau lagoon in the context of the 2011-2016 WFD diagnosis (concentrations measured: 0.2, 0.2, 22.2, 0.9 µmol.l^{-1} respectively) (Derolez

et al., 2017). DIN p90 were significantly higher (Kruskal-Wallis, p-value < 0.001) in 2015 (mean = 0.49) than in 2014 and 2016 (mean: 0.31 and 0.33, respectively), regardless of the scenario tested.

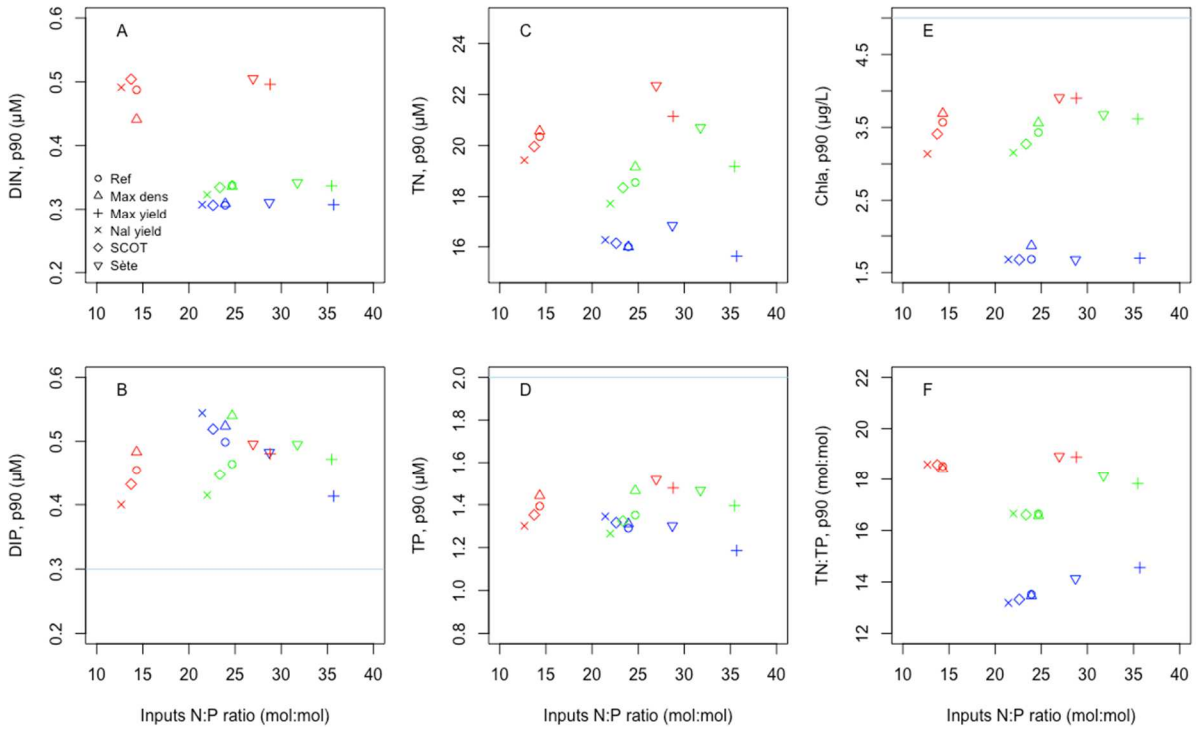

Figure 7. 90th percentiles for DIN (A), DIP (B), TN (C), TP (D), Chl *a* (E) and TN:TP ratio (F) as a function of inputs N:P molar ratio for all scenarios (see legend in Figure A inset). Colors correspond to simulated years (2014: blue, 2015: red, 2016: green). High/Good ecological status thresholds according to WFD are represented by blue lines for DIP, TP and Chl *a*. These thresholds were not visible for DIN (2 µM) and TN (50 µM).

TN p90 were contrasted between years with significant differences recorded between 2014 and the two other years 2015 and 2016 (Kruskal-Wallis, p-value < 0.001). Finally, Chl *a* p90 were found significantly lower (Kruskal-Wallis, p-value < 0.001) in 2014 (mean = 1.71 µg.l^{-1}) than 2015 and 2016 (mean = 3.60 and 3.45 µg.l^{-1}, respectively).

However, the model seemed to underestimate TN values (17.6 and 20.4 µmol.l^{-1} for the "Reference" scenario, n=92 and all scenarios, n=552, respectively). Nitrogen and Phosphorus inputs, associated with the different scenarios, did not seem to affect the ecological diagnosis

of the water column based on nutrient indicators as none of these scenarios triggered a modification of ecological status classes. These simulated indicators gave p90 values in agreement with the "High" status fixed by WFD (MEDDE, 2015), in accordance with the High status evaluated by 2011-2016 WFD diagnosis. Only simulated DIP concentrations were classified in the “good” ecological status for all scenarios (Table 2). Shellfish production at harvest, for all scenarios, decreased significantly for a given year when the N:P ratio of catchment contributions increased (Figure 8-A). These relationships have a Spearman correlation coefficient of -0.75, -0.98 and -0.90 for years 2014, 2015 and 2016 respectively (p-value <0.05 for the three relationships) although no significant relationship has been established between shellfish production and nitrogen inputs or phosphorus inputs independently.

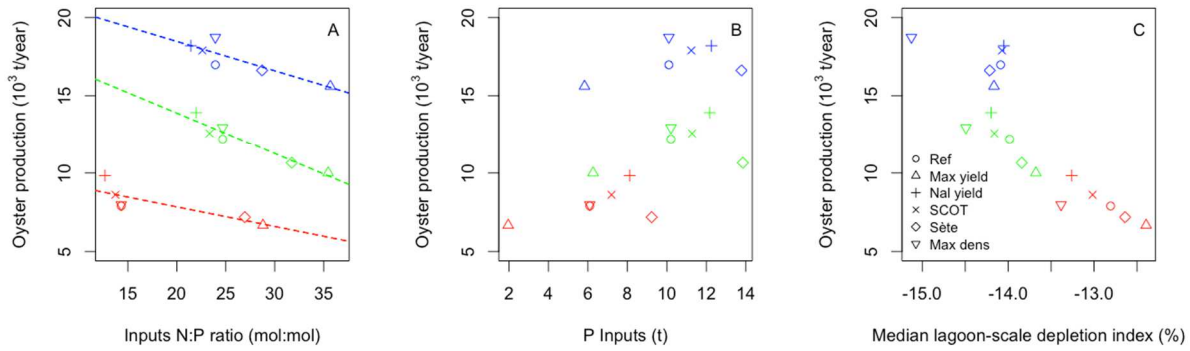

Figure 8. Oyster production as a function of (A) inputs N:P ratio, (B) phosphorus inputs and (C) median lagoon-scale depletion index for the three years (2014: blue, 2015: red, 2016: green) and all scenarios (see legend inset).

In addition, production was negatively correlated with the median lagoon-scale depletion index, but this relationship was not linear for a given year (Fig. 8-B).

The "Max. Dens." Scenario (n°6) had the lowest median depletion index (Figure 8-B) indicating that it had more impact on phytoplankton biomass than scenarios with comparable production outputs (ie "Nal Yield", scenario n°3). On the other hand, the "Max. yield" (n°2) and "Sète" (n°5) scenarios gave the highest median depletion indexes but at the expense of

lower oyster productions. The comparison of nitrogen and phosphorus quantities added to the lagoon in each of the three simulated years showed the role of the hydro-meteorology on oyster production.

4 Discussion

The GAMELag-Conch model was developed to address the questions related to the management of the Thau lagoon ecosystem with regards to the issues of shellfish production and ecological status regulations. Scenarios tested were developed from realistic management hypotheses. These hypotheses included leverages on the quantities of nitrogen and phosphorus potentially available through waste water treatment plant management or on the quantities of cultured filter feeders introduced in farming zones.

4.1 Scenarios and oyster performances

All scenarios tested in this study were based on achievable management objectives. In this respect, little difference was highlighted from oyster performance model outputs when comparing scenarios. Although, nutrient loadings, in terms of nitrogen and phosphorus, were varying with these different scenarios, the highest increase in oyster production was recorded at +25% ("Normal yield" scenario) in 2015 in comparison to "Reference". This specific case corresponded to the modification of the Mèze WWTP efficiency, going from maximum to normal abatements, and a very dry year (2015, - 200 mm) where WWTP effluents were the main contributors to nutrient loadings (+7 t N and +2 t P). To a lesser extent, "SCOT" and "Max. density" scenarios also demonstrated an increase in oyster production but limited to +3 to +9% and +1 to +10%, respectively. The effect of increased nutrient loadings, mainly nitrogen, on the production of cultured filter feeders has already been reported in modelling studies (Ferreira et al., 2007; Guyondet et al., 2014; Rose et al., 2015). On the opposite,

661 reducing nutrient loadings from the watershed (scenario “Max yield” in this study) through
662 the improvement of waste water treatment efficiency triggered a loss in production between -
663 8% and -18% compared to our “Reference” scenario further indicating this dependence of
664 oyster farming on nutrient supply of the Thau system. However, the variation in nutrient
665 loadings quantity may not solely explain the response of cultured oyster as large addition of
666 nitrogen (+171%) in the “Sète” scenario rendered lower oyster production than “Reference” (-
667 2% to -13%). This effect is probably linked to the joint influence of nitrogen and phosphorus
668 additions, the location of these inputs and the response of the biological compartments and is
669 further discussed below. In terms of oyster performances, scenarios associated with increased
670 nutrient loadings demonstrated that oysters marginally gained in length, quality (condition
671 index) and total weight at harvest but remained in the same market grade (66-85 g; according
672 to the French 6 grades weight where n°5: 30-45g, n°4: 46-65g, n°3:66-85g, n°2: 86-110g, n°1:
673 111-150g and n°0: over 151g). However, a reduction of, as well as unbalanced, nutrient
674 loadings, produced smaller oysters and a modification of the market grade (46-65 g) with
675 potential repercussion on economic aspects (Ferreira et al., 2007). Finally, “Max. density”
676 scenario demonstrated higher oyster production but at the expenses of thinner oysters with
677 lower condition index. This scenario highlighted the density effect where an increased
678 abundance triggered a competition for the resources yielding smaller individuals (Gangnery et
679 al., 2001; Gangnery, 2003; Filgueira et al., 2014b).
680 The scenarios tested here have revealed differences in terms of oyster performances and
681 productions, however, major contrasts were brought by interannual variability where dry
682 against wet years triggered the largest variations in nutrient loadings. Consequently, oyster
683 productions were significantly lower in years presenting evident rainfall deficit. Oyster
684 lengths, total weight and condition index were also significantly affected with smaller, lighter
685 and lower quality during dry years. Nevertheless, oyster production and performances

686 evaluated through this modelling work shall be replaced within the context of ecological
687 status and ecological carrying capacity to better assess overall functioning of the ecosystem
688 (Byron et al., 2011b; Higgins et al., 2011).
689
690 4.2 Trophic carrying capacity and ecological status
691 One of the objectives of this work was to assess the carrying capacity of the Thau lagoon
692 regarding to shellfish farming within the frame of WFD regulation. The Thau lagoon, as any
693 other shellfish farming sites, is characterized by complex dynamics of interacting biological
694 and physical processes. Within these systems, filter feeding activity may deeply modify the
695 energy fluxes as they clear large volume of water including suspended particles (Dowd, 2003;
696 Filgueira et al., 2014a).
697 To evaluate the capability of an ecosystem to support various uses, it is important to compare
698 phytoplankton production, phytoplankton biomass, lagoon hydrodynamics as well as shellfish
699 culture pressure to truly highlight the limits of the ecosystem. A first approach using these
700 different aspects of the functioning of the ecosystem is the Dame index (Dame and Prins.,
701 1998). This index relates the characteristic times RT (renewal time), CT (clearance time) and
702 PPT (phytoplankton biomass renewal time) of the Thau lagoon. The CT:RT ratio indicates
703 whether filter feeders and its resources are controlled by exchanges with the sea or by internal
704 (including inputs from the watershed) availability of nutrients. The GAMELag-Conh model
705 was able to simulate oyster productions along with indicators of the ecological status,
706 depletion index and characteristic times (CT, RT, PPT) comparatively with different scenarios
707 of nutrient inputs and shellfish cultures. The relationships between oyster production and the
708 carrying capacity of the lagoon was evaluated with regards to the Dame index, particularly the
709 CT:PPT ratio, and the lagoon-scale phytoplankton depletion index. Both markers
710 demonstrated a top-down control of filter feeders on phytoplankton population. In this study,

711 simulated clearance and water renewal times, CT and RT, indicated that hydrodynamic
712 exchanges with the far field (outside the lagoon) were not efficient enough to drive the filter
713 feeder resources. Therefore, phytoplankton dynamic or its bottom-up control, would rather be
714 driven by nutrients coming from the watershed. In comparison, the Marennes-Oléron site
715 (Bacher, 1989; Dame and Prins., 1998; Raillard and Menesguen, 1994) showed slower
716 phytoplankton biomass renewal times and much faster filtration capacity resulting in a system
717 that did appear to be largely under pressure (Marennes-Oléron CT:PPT = 0.27) despite a more
718 efficient hydrodynamics than in the Thau lagoon (Marennes-Oléron RT = 7.1). The simulated
719 values of the CT:PPT ratio suggested that the consumption of phytoplankton biomass by
720 farmed oysters was constrained between 34 and 50%, leaving half, or more, of the
721 phytoplankton stock available for other trophic levels. Trousselier & Deslous-Paoli (2001)
722 had also concluded that Thau lagoon was productive in the 1990s, with shellfish harvested
723 production representing about 3% of primary production. Dame and Prins (1998) postulated
724 that successful shellfish population occur when RT is less than 40 days and PPT below 4
725 days. If characteristic times calculated for the Thau lagoon are longer than these
726 recommended times, shellfish cultures have prospered in the Thau lagoon and its carrying
727 capacity did not seem to be threatened. Both ratios, CT:RT and CT:PPT, expressed the state
728 of the carrying capacity of the lagoon by comparing the characteristic times of physics,
729 phytoplankton, and shellfish in culture (Table 2). However, they do not consider the presence
730 of nutritive resources other than phytoplankton such as zooplankton or particulate organic
731 matter. The model outputs indicated that oyster production is related to the input N:P molar
732 ratio with production increasing with decreasing N:P ratios. These linear relationships were
733 contrasted between years, highlighting the strong influence of the hydrological regime and
734 hence the quantities of nitrogen and phosphorus entering the lagoon. These first relationships
735 were bounded by the maximum WWTP yield and normal WWTP yield scenarios as they

736 provided the highest and lowest input N:P molar ratio, respectively. This also revealed that, if
737 filter feeder production might be increased by decreasing the N:P ratio of inputs, the amount
738 of nutrients coming from the watershed, most probably phosphorus, would limit the
739 maximum levels of production to be reached. The shellfish productions were also increasing
740 with decreasing lagoon-scale depletion index indicating that more production would trigger
741 higher depletion of the Thau system. Once again, the most apparent contrast was linked to the
742 different simulated years where higher nutrient loadings generated higher shellfish
743 productions and hence an increased pressure on its phytoplankton resource. N:P ratio of
744 loadings, however, was similar in 2014 and 2016, whereas phytoplankton summer biomass
745 was similar in 2015 and 2015. Therefore, higher oyster production and subsequent increased
746 filter feeder pressure could not only be explained by nutrient loadings. Annual mean
747 temperature anomaly, compared to the 1970-2016 mean (15.3°C) was +1.5°C, +1.4°C and
748 +1.1°C for 2014, 2015 and 2016 respectively. In previous modelling studies (Filgueira et al.,
749 2016), increased temperature has been identified as a key factor in enhancing grazer activity
750 through higher metabolism with concomitant higher pressure on phytoplankton. The highest
751 oyster production simulated in 2014 would be in agreement with highest annual average
752 temperature recorded in 2014 for the Thau lagoon. In addition, 2015 was associated with low
753 nutrient inputs, which resulted in low oyster performances, even if temperature anomaly was
754 similar to 2014. In this second relationship (e.g. oyster production against depletion index),
755 oyster production was bounded by the maximum oyster densities and the maximum WWTP
756 yield scenarios. The use of maximum allowed stocking densities generated the highest
757 depletion in agreement with the density effect (Chapelle et al., 2000; Grant et al., 2007;
758 Grangeré et al., 2010).
759 The increase in the quantities of seeded shellfish did not lead to significantly higher harvests
760 compared to the “Reference” scenario (1 to 10%). Moreover, the shellfish thus produced were

761 smaller, probably because of the competition for the nutritive resource between growing
762 individuals. This scenario also exhibited the lowest CT:PPT ratios indicating a noticeable
763 pressure of farmed oysters on their phytoplankton resource. Accordingly, highest depletion
764 was recorded when increasing stocking densities, which corroborates this impact on
765 phytoplankton stock. However, Chl *a* concentrations, used in the ecological status evaluation,
766 were not lower in the presence of higher densities of filter feeders than with the other
767 scenarios. This might be explained either by the fact that: 1) energy stocks of filter feeders
768 during the summer are allocated to spawning rather than nutrition (e.g. filtration), or 2) the
769 increase in cultured bivalve density may have a positive feedback effect on phytoplankton
770 outside growing structures through more excretion of inorganic nutrients (Filgueira et al.,
771 2014b; Kellogg et al., 2014).
772 It is important to note that shellfish farming activities occupy about 20% of the Thau lagoon
773 area (~ 30% by volume) which is probably a criterion of its durability. In agreement with the
774 occupational state of the Thau lagoon, Byron et al (2011b) reported, using the Ecopath model
775 on the Narragansett bay, another example of a low-intensity of shellfish cultures where
776 carrying capacity is not reached due to high nutrient loadings and primary productivity. These
777 authors evaluated that if shellfish cultures density remained at current levels, the growing area
778 might theoretically be extended up to 26% of the bay area without exceeding the ecological
779 carrying capacity. On the contrary, the study by Filgueira et al. (2014), concerning a bay
780 occupied at 80% in volume by the mussel farms, showed a strong impact on the
781 phytoplankton resource, where the median bay-scale depletion index (-34.2%) was below the
782 sustainable threshold calculated from natural variability of Chl *a* concentration (-27.5%). This
783 shellfish farming pressure was also reported, to a lesser extent, in Saint Peter's Bay
784 (Guyondet et al, 2015), where only the central part of the bay exhibited depletion for a total
785 farmed area of 40%.

786 The simulated ecological indicators were chosen to correspond to the observations used in the
787 WFD diagnosis (EC, 2000). Regardless of scenarios or simulated years, these ecological
788 indicators fell into the “high” ecological status class. Only, simulated DIP concentrations
789 exceeded the “high” to “good” threshold (0.3 µM), hence placing the ecological status of the
790 lagoon into the “good” conditions for the water column chemistry. The comparison of
791 simulated years or scenarios showed significant differences for DIN between dry and wet
792 years with higher concentrations recorded during the dry year (2015) and for Chl *a* where
793 concentrations in 2015 and 2016 were found higher than in 2014. The main concluding
794 remarks on this ecological status evaluation is that scenarios tested in this study did not
795 altered the ecological status of the lagoon. In addition to this fulfilling “high” ecological
796 status, weak phytoplankton depletion and the moderate pressure of cultured oysters on their
797 resources, the current oyster production (“Ref”, scenario n°1), oscillating between 7900 and
798 17000 tons, would therefore be sustainable and not conflicting with EU regulation nor are
799 opposed to the important efforts made to reduce nutrient inputs from the watershed. Indeed,
800 ecological carrying capacity appears as a major component in the evaluation of the whole
801 ecosystem functioning and should be carefully considered at the same level as ecological
802 status.
803
804 4.3 Control of lagoon phytoplankton and shellfish productivity
805 The results obtained in this modeling work of the Thau lagoon seemed to indicate a control of
806 the system by the nitrogen and phosphorus inputs from the watershed and more precisely by
807 the N:P ratio of these inputs. When the inputs related to the various scenarios are detailed, it
808 appeared that if the N inputs from the watershed covered a wide range of values (25.5 to
809 198.6 tons), the variability of phosphorus inputs was much smaller (1.8 to 13.8 tons). The
810 variability of N and P inputs related to the hydrometeorological regime seemed the main

811 driver for the variability of shellfish production. Increases of 57% and 27% in N and P inputs
812 during wet years led to a 36% increase in predicted oyster production.
813 By replacing shellfish production at harvest in the context of nitrogen and phosphorus inputs
814 for all scenarios and the three simulated years, an optimum of the N:P inputs molar ratio
815 appeared (~ 18.4) around which the oyster productions seemed to be maximized (in 2014 and
816 2016, wet years). Current loadings ("Reference"), both natural and anthropogenic, are just
817 over 100 tons of nitrogen in wet years (2014, 2016) for a phosphorus input of about 10 tons,
818 bringing the N:P molar ratio above 22. To obtain a molar ratio of inputs around 18.4, it would
819 therefore be necessary to bring an additional 2.5 tons of P into the system (ie 12.5 tons of P in
820 total). Phosphorus appeared to be insufficient and therefore limiting if one considers these
821 current contributions of nitrogen. The "Sète" scenario (n° 5) confirmed the hypothesis of a
822 phosphorus-controlled system, where a misleading excess of nitrogen (~ +100 tons) did not
823 help to achieve higher production because this scenario increased the phosphorus deficit in
824 the system. Although more P was brought to the lagoon, oyster production did decrease in
825 comparison with "reference" scenario. The "Sète" scenario tested the response of the
826 ecosystem to excess N and P loading from a WWTP. In the current situation, this WWTP
827 releases its wastewater into the sea. This scenario involved the release of waste waters into
828 box 1 ("Petit étang") of the model. Box 1 is the box connected with the sea, hence part of
829 these inputs is exchanged with the sea, the other part reached box 2 then box 3 where cultured
830 areas are located. In the "Sète" scenario, the model shows that sediment has accumulated
831 more N (times 2.5) and has released less P (times 0.4) in box 1 than the "Reference". Along
832 with the sediment compartment, macroalgae, notably Ulva and Gracilaria, yielded higher
833 biomasses (times 2 and times 1.5 for Ulva and Gracilaria respectively) than in the reference
834 scenario. This may indicate that macrophytes enter a competition for nutrients in box 1. N &
835 P in sediment and macroalgae did not show marked differences in all other boxes of the

836 model. Nevertheless, this would indicate that box 1 was the first to respond to these additional
837 inputs. Remaining nitrogen and phosphorus were then exchanged with the sea and with box 2
838 and further up. Macrophytes competing for nutrient resources and a greater accumulation of
839 matter may have led to a lower P availability in boxes 2 and 3 including farming areas (boxes
840 4 and 5) and hence lower oyster production.
841 N inputs (N), P inputs (P) and N:P ratio of inputs (NP) were used in a PCA analysis (Figure 9)
842 along with shellfish culture performances variables such as production (Prod), total weight at
843 harvest (P_tot) or condition index (CI) and ecosystem functioning variables as chlorophyll *a*
844 concentration in and out oyster farming zones (Chla_OF and Chla_out, respectively) or the
845 lagoon-scale phytoplankton depletion index (DI). Phosphorus inputs were strongly correlated
846 with shellfish performances (first axis, 71.51% of variance explained) and chlorophyll *a*
847 concentrations, suggesting a key role of phosphorus in controlling both phytoplankton and
848 oyster production.

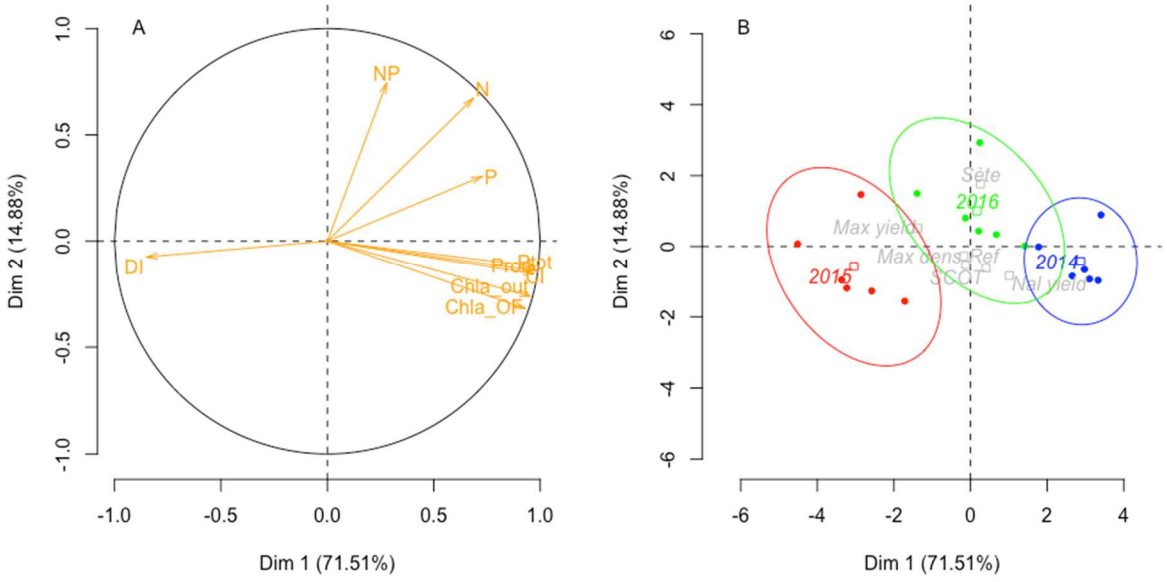

849

850 Figure 9. PCA analysis (A) of model outputs including nitrogen inputs (N), phosphorus inputs (P),
851 inputs N:P ratio (NP), oyster production (Prod), oyster total weight (P_tot), condition index (CI), Chl a
852 concentration in (Chla_OF) and outside (Chla_out) oyster farms and the median lagoon-scale
853 phytoplankton depletion index (DI). Supplementary qualitative variables (B) representing simulated

854 years with coloured 95% confidence interval ellipses (individuals: dots and barycentre: square) and
855 scenarios (named grey squares).
856
857 The phosphorus inputs were inversely correlated with the depletion index, indicating also a
858 role in regulating the carrying capacity of the Thau lagoon. Nitrogen to phosphorus ratio of
859 inputs, and to a lesser extent nitrogen inputs, explained the second dimension of this PCA
860 analysis (14.88% of variance explained; Figure 9-A) suggesting that, if phosphorus may
861 control production levels importantly, the balance between nitrogen and phosphorus in
862 loadings carried from the watershed had a major importance in the efficiency of the Thau
863 ecosystem and hence on its trophic carrying capacity. Supplementary variables, as simulated
864 years and simulated scenarios, once placed in this PCA (Figure 9-B), demonstrated the major
865 importance of contrasted hydrological conditions as suggested above, whereas the variability
866 linked to the scenarios tested in this study exhibited less difference between scenarios with no
867 clear pattern.
868 Deslous-Paoli et al. (1998) reported this control of shellfish production by phosphorus in the
869 1990s, where the oyster stocking density was around 25 to 30 000 tons of shellfish and for an
870 annual production exceeding 15 000 tons (against 9200 to 9500 tons currently reported by
871 shellfish farmers). This study also reported phosphate concentrations in water 40 times higher
872 than the current concentrations (4 μM against 0.1 μM). At the same time, even though the
873 concentrations of PO_4^{3-} in water have been decreasing since the 1970s, the significant
874 expansion of oyster farming during this period (from 1400 to 2440 tables in 20 years) would
875 have reduced the risk of eutrophication by removing about 30%, according to the authors, of
876 this readily available phosphorus from the Thau lagoon. At present, the decrease in
877 phosphorus inputs from the watershed and, consequently, the concentrations in the water
878 column, is mainly attributed to the major efforts made on the waste water treatment systems
879 (Derolez et al., 2013; La Jeunesse, 2001; Souchu et al., 2010). Depending on the year, the

880 contribution of anthropogenic inputs from WWTP varies importantly to supply up to 90% of
881 total inputs in dry years. The N:P molar ratio of these anthropogenic inputs (~5; 2009-2016
882 average, data not shown) is much lower than that of natural inputs (~40; 2009-2016 average,
883 data not shown), thus placing the lagoon in nitrogen limiting conditions in those years, the
884 main source of current phosphorus inputs coming from the WWTPs.
885
886 5 Conclusions
887 The GAMELag-Conch model, developed to answer the problem of reconciling resource
888 exploitation through shellfish culture and regulatory constraints, allowed an evaluation of the
889 ecosystem carrying capacity of the Thau lagoon and the simulation of various scenarios waste
890 water treatment management and shellfish farming strategies. To the best of our knowledge,
891 there are no existing model taking into account both nitrogen and phosphorus inputs within
892 the frame of carrying capacity assessment and most carrying capacity models are based solely
893 on nitrogen (Dowd, 2003; Byron et al., 2011c; Chapelle et al., 2000; Filgueira et al., 2014a;
894 Guyondet et al., 2014) or biomass data sets (Jiang and Gibbs, 2005). Under current
895 conditions, the carrying capacity of the Thau Lagoon does not appear to be limiting. The
896 interannual variability introduced by the differences in weather conditions strongly affects
897 shellfish farming in terms of production and shellfish performances rather than did the
898 contrast between the different tested scenarios. The productivity of the ecosystem seemed to
899 depend mainly on watershed inputs in which inputs from WWTPs had a predominant role in
900 dry years. Shellfish production was more specifically controlled by phosphorus as revealed by
901 unbalanced N:P ratio in loadings. The trophic resource being sufficient, the oyster control on
902 the phytoplankton was not excessive and depended on the stock density of cultured bivalves
903 or additional phosphorus brought to the lagoon. The use of high stocking densities should be
904 prohibited because if they generated higher production than current conditions, at the

905 expenses of thinner oysters with low condition index. Finally, the ecological status did not
906 appear to be threatened with regard to the current shellfish pressure. This model thus appeared
907 as a suitable tool for management perspectives. Another strength and recommended approach
908 (Byron et al., 2011a) of this work resides in the implication of shellfish farmers, stakeholders,
909 local and governmental management bodies as well as scientists to implement realistically
910 based scenarios in the search for an equilibrium between shellfish production and ecological
911 status regulation.
912 However, important caveats must be given here as this paper reports a global evaluation of the
913 carrying capacity through the use of characteristic times or depletion index that might vary in
914 time and space (Dame and Prins., 1998; Guyondet et al., 2014). Further work is necessary to
915 alleviate this time varying control of the carrying capacity where characteristic times or even
916 depletion index are used to identify seasonal effects and sensitive periods to be confronted to
917 shellfish production, performances and potential ecological impacts. This ongoing work shall
918 help management of shellfish culture practices in this context of maintaining “good”
919 ecological status. A perspective use of this numerical tool resides in a theoretical approach
920 that would involve large variations of nutrient loadings to seek for tipping points where
921 depletion or ecological indicators may drastically change with strong impacts on the whole
922 ecosystem functioning. Short term development of this tool would address the question of
923 anoxic crisis, which had sporadically occurred in the Thau lagoon when temperature increases
924 and weather conditions are calm. These anoxic crises have led to dramatic loss of cultured
925 bivalves hence temporarily damaging ecological conditions of the lagoon. Further
926 developments of this management tool should address questions related to climate change,
927 where the frequency and-or the intensity of meteorological events, such as temperature
928 increase or the modification of rainfall regimes should be considered concomitantly with

929 increase in population, in turn increasing watershed loadings, subsequent refit of WWTP and
930 sustainability of uses in the Thau lagoon.
931
932 ## 6 Acknowledgements
933 This study was supported by the University of Montpellier, Ifremer and DLAL-FEAMP
934 (CAPATHAU postdoctoral fellowship). The authors thank Melaine Gourault for providing
935 the latest version of the DEB model for *Crassostrea gigas*. Thanks to Eve Mouret for
936 adapting this model to the Thau Lagoon oysters as part of her Master thesis, and Christophe
937 Lett for his help in her supervision. We express our gratitude to all the staff of the LER-LR
938 laboratory, involved in the observation networks of the REPHY, the RESCO, the RSL-DCE,
939 specifically Claude Chiantella, Eric Abadie, Clarisse Hubert, Serge Mortreux, Patrik le Gall,
940 Gregory Messiaen, Anais Crottier, Elodie Foucault, Martine Fortune, Dominique Munaron,
941 Tom Berteaux, Jocelyne Oheix, Emmanuelle Roque d'Orbcastel and the coordinators of these
942 networks (Catherine Belin, Elodie Fleury, Valérie derolez). Our thanks also go to the SMBT
943 for providing the database of nitrogen and phosphorus inputs from the watershed. The authors
944 also thank the DLAL animators (Beatrice Pary, Agnes D'Artigues) and the people involved in
945 the scenario construction (SMBT: Luc Hardy, David Cottalorda, CRCM: Denis Regler,
946 Adeline Perignon, Cepralmar: Matthew Hebert, Erika Gervasoni, Anahita Marzin, DDTM:
947 Philian Retif, AERMC: Anahi Barrera, Anais Giraud).
948
949 ## 7 References
950 Alunno-Bruscia, M., Bourlès, Y., Maurer, D., Robert, S., Mazurié, J., Gangnery, A.,
951 Goulletquer, P., Pouvreau, S., 2011. A single bio-energetics growth and reproduction model
952 for the oyster *Crassostrea gigas* in six Atlantic ecosystems. J. Sea Res. 66, 340–348.
953 https://doi.org/10.1016/j.seares.2011.07.008

954 Bacher, C., 1989. Capacité trophique du bassin de Marennes-Oléron : couplage d'un modèle
955 de transport particulaire et d'un modèle de croissance de l'huître *Crassostrea gigas*. Aquat.
956 Living Resour. 2, 199–214. https://doi.org/10.1051/alr:1989025
957 Bacher, C., Duarte, P., Ferreira, J.G., Héral, M., Raillard, O., 1998. Assessment and
958 comparison of the Marennes-Oléron Bay (France) and Carlingford Lough (Ireland) carrying
959 capacity with ecosystem models. Aquat. Ecol. 31, 379–394.
960 https://doi.org/10.1023/A:1009925228308
961 Bec, Béatrice, Valérie Derolez, Dominique Soudant, Ludovic Cesmat, Romain Pete, and
962 Marion Richard. 2018. Projet CAPATHAU : Capacité Trophique de la lagune de Thau.
963 Evolution temporelle de l'état écologique de la lagune de Thau et des performances des
964 coquillages en élevage au regard de la réduction des apports issus du bassin versant et des
965 changements météo. 58 p.
966 Bernard, I., de Kermoysan, G., Pouvreau, S., 2011a. Effect of phytoplankton and temperature
967 on the reproduction of the Pacific oyster *Crassostrea gigas*: Investigation through DEB
968 theory. J. Sea Res. 66, 349–360. https://doi.org/10.1016/j.seares.2011.07.009
969 Bernard, I., de Kermoysan, G., Pouvreau, S., 2011b. Effect of phytoplankton and temperature
970 on the reproduction of the Pacific oyster *Crassostrea gigas*: Investigation through DEB
971 theory. J. Sea Res. 66, 349–360. https://doi.org/10.1016/j.seares.2011.07.009
972 Bougrier, S., Geairon, P., Deslous-Paoli, J.M., Bacher, C., Jonquières, G., 1995. Allometric
973 relationships and effects of temperature on clearance and oxygen consumption rates of
974 *Crassostrea gigas* (Thunberg). Aquaculture 134, 143–154. https://doi.org/10.1016/0044-
975 8486(95)00036-2
976 Bourlès, Y., Alunno-Bruscia, M., Pouvreau, S., Tollu, G., Leguay, D., Arnaud, C.,
977 Goulletquer, P., Kooijman, S. a L.M., 2009. Modelling growth and reproduction of the Pacific
978 oyster *Crassostrea gigas*: Advances in the oyster-DEB model through application to a coastal

979 pond. J. Sea Res. 62, 62–71. https://doi.org/10.1016/j.seares.2009.03.002
980 Brigolin, D., Maschio, G.D., Rampazzo, F., Giani, M., Pastres, R., 2009. An individual-based
981 population dynamic model for estimating biomass yield and nutrient fluxes through an off-
982 shore mussel (*Mytilus galloprovincialis*) farm. Estuar. Coast. Shelf Sci. 82, 365–376.
983 https://doi.org/10.1016/j.ecss.2009.01.029
984 Byron, C., Bengtson, D., Costa-Pierce, B., Calanni, J., 2011a. Integrating science into
985 management: Ecological carrying capacity of bivalve shellfish aquaculture. Mar. Policy 35,
986 363–370. https://doi.org/10.1016/j.marpol.2010.10.016
987 Byron, C., Link, J., Costa-Pierce, B., Bengtson, D., 2011b. Calculating ecological carrying
988 capacity of shellfish aquaculture using mass-balance modeling: Narragansett Bay, Rhode
989 Island. Ecol. Modell. 222, 1743–1755. https://doi.org/10.1016/j.ecolmodel.2011.03.010
990 Byron, C., Link, J., Costa-Pierce, B., Engtson, D., 2011c. Modeling ecological carrying
991 capacity of shellfish aquaculture in highly flushed temperate lagoons. Aquaculture 314, 87–
992 99. https://doi.org/10.1016/j.aquaculture.2011.02.019
993 Carver, C.E.A., Mallet, A.L., 1990. Estimating the carrying capacity of a coastal inlet for
994 mussel culture. Aquaculture 88, 39–53. https://doi.org/10.1016/0044-8486(90)90317-G
995 Chapelle, A., Ménesguen, A., Deslous-Paoli, J.M., Souchu, P., Mazouni, N., Vaquer, A.,
996 Millet, B., 2000. Modelling nitrogen, primary production and oxygen in a Mediterranean
997 lagoon. Impact of oysters farming and inputs from the watershed. Ecol. Modell. 127, 161–
998 181. https://doi.org/10.1016/S0304-3800(99)00206-9
999 Dabrowski, T., Lyons, K., Curé, M., Berry, A., Nolan, G., 2013. Numerical modelling of
1000 spatio-temporal variability of growth of *Mytilus edulis* (L.) and influence of its cultivation on
1001 ecosystem functioning. J. Sea Res. 76, 5–21. https://doi.org/10.1016/j.seares.2012.10.012
1002 Dame, R.E., Prins., T.C., 1998. Bivalve carrying capacity in coastal ecosystems. Aquatic
1003 Ecology 31(4):409-421. 409–421.

1004 Derolez, V., Ouisse, V., Fiandrino, A., Munaron, D., Bissery, C., Kloareg, M., 2013. Analyse
1005 statistique des données du RSL - Etude des trajectoires écologiques des lagunes entre 2001 et
1006 2012.
1007 DDTM. 2014. Arrêté n° DDTM34-2016-06-04069 du 19 juin 2014 portant Schéma des
1008 structures des autorisations d'exploitation de cultures marines situées dans le Département de
1009 l'Hérault. http://www.cepralmar.org/guide_conchylicole/documents/2.1.2-
1010 Structures_Herault.pdf
1011 Deslous-Paoli, J.M., Souchu, P., Mazouni, N., Juge, C., Dagault, F., 1998. Relations milieu-
1012 ressources: Impact de la conchyliculture sur un environnement lagunaire Mediterraneen
1013 (Thau). Oceanol. Acta 21, 831–843. https://doi.org/10.1016/S0399-1784(99)80010-3
1014 Dowd, M., 2003. Seston dynamics in a tidal inlet with shellfish aquaculture: A model study
1015 using tracer equations. Estuar. Coast. Shelf Sci. 57, 523–537. https://doi.org/10.1016/S0272-
1016 7714(02)00397-9
1017 European Community, 2000. Directive 200/60/EC of the European parliament and of the
1018 council of 23 October 2000 establishing a framework for community action in the field of
1019 water policy.
1020 European Community, 1991, Council Directive 91/676/EEC of 12 December 1991
1021 concerning the protection of waters against pollution caused by nitrates from agricultural
1022 sources.
1023 European Community, 2004. Case C-280/02. Commission of the European Communities v
1024 French Republic. Failure of a Member State to fulfil obligations – Directive 91/271/EEC.
1025 Urban waste water treatment. Article 5(1) and (2) and Annex II. Failure to identify sensitive
1026 areas. Meaning of "eutrophication". Failure to implement more stringent treatment of
1027 discharges into sensitive areas. https://eur-lex.europa.eu/legal-
1028 content/EN/TXT/HTML/?uri=CELEX:62002CJ0280&from=FR

Fao, 2018. World Fisheries and Aquaculture, Aquaculture. https://doi.org/issn 10

Ferreira, J.G., Hawkins, A.J.S., Bricker, S.B., 2007. Management of productivity, environmental effects and profitability of shellfish aquaculture - the Farm Aquaculture Resource Management (FARM) model. Aquaculture 264, 160–174. https://doi.org/10.1016/j.aquaculture.2006.12.017

Ferreira, J.G., Hawkins, A.J.S., Monteiro, P., Moore, H., Service, M., Pascoe, P.L., Ramos, L., Sequeira, A., 2008. Integrated assessment of ecosystem-scale carrying capacity in shellfish growing areas. Aquaculture 275, 138–151. https://doi.org/10.1016/j.aquaculture.2007.12.018

Fiandrino, A., Giraud, A., Robin, S., & Pinatel, C. (2012). Validation d'une méthode d'estimation des volumes d'eau échangés entre la mer et les lagunes et définition d'indicateurs hydrodynamiques associés.

Fiandrino, A., Ouisse, V., Dumas, F., Lagarde, F., Pete, R., Malet, N., Le Noc S., de Wit, R. (2017). Spatial patterns in coastal lagoons related to the hydrodynamics of seawater intrusion. Marine Pollution Bulletin, 119(1), 132–144. http://doi.org/10.1016/j.marpolbul.2017.03.006

Filgueira, R., Comeau, L. a, Guyondet, T., Mckindsey, C.W., Byron, C.J., 2015. Modelling carrying capacity of bivalve aquaculture: A review of definitions and methods, Encyclopedia of Sustainability Science and Technology. https://doi.org/10.1007/978-1-4939-2493-6

Filgueira, R., Grant, J., 2009. A box model for ecosystem-level management of mussel culture carrying capacity in a Coastal Bay. Ecosystems 12, 1222–1233. https://doi.org/10.1007/s10021-009-9289-6

Filgueira, R., Guyondet, T., Comeau, L. a., Grant, J., 2014a. A fully-spatial ecosystem-DEB model of oyster (*Crassostrea virginica*) carrying capacity in the Richibucto Estuary, Eastern Canada. J. Mar. Syst. 136, 42–54. https://doi.org/10.1016/j.jmarsys.2014.03.015

Filgueira, R., Guyondet, T., Comeau, L.A., Grant, J., 2014b. Physiological indices as indicators of ecosystem status in shellfish aquaculture sites. Ecol. Indic. 39, 134–143.

https://doi.org/10.1016/j.ecolind.2013.12.006

Filgueira, R., Guyondet, T., Comeau, L.A., Tremblay, R., 2016. Bivalve aquaculture-environment interactions in the context of climate change. Glob. Chang. Biol. 22, 3901–3913. https://doi.org/10.1111/gcb.13346

Gangnery, A., 2003. Etude et modélisation de la dynamique des populations de bivalves en élevage (*Crassostrea gigas* et *Mytilus galloprovincialis*) dans le bassin de Thau (Méditerranée, France) et des ascidies solitaires associées. Phd Thesis 1–175.

Gangnery, A., Bacher, C., Buestel, D., 2001. Assessing the production and the impact of cultivated oysters in the Thau lagoon (Mediterranee, France) with a population dynamics model. Can. J. Fish. Aquat. Sci. 58, 1012–1020. https://doi.org/10.1139/f01-028

Grangeré, K., Lefebvre, S., Bacher, C., Cugier, P., Ménesguen, A., 2010. Modelling the spatial heterogeneity of ecological processes in an intertidal estuarine bay: Dynamic interactions between bivalves and phytoplankton. Mar. Ecol. Prog. Ser. 415, 141–158. https://doi.org/10.3354/meps08659

Grangeré, K., Ménesguen, A., Lefebvre, S., Bacher, C., Pouvreau, S., 2009. Modelling the influence of environmental factors on the physiological status of the Pacific oyster *Crassostrea gigas* in an estuarine embayment; The Baie des Veys (France). J. Sea Res. 62, 147–158. https://doi.org/10.1016/j.seares.2009.02.002

Grant, J., Curran, K.J., Guyondet, T.L., Tita, G., Bacher, C., Koutitonsky, V., Dowd, M., 2007. A box model of carrying capacity for suspended mussel aquaculture in Lagune de la Grande-Entrée, Iles-de-la-Madeleine, Québec. Ecol. Modell. 200, 193–206. https://doi.org/10.1016/j.ecolmodel.2006.07.026

Grant, J., Filgueira, R., 2011. The application of dynamic modelling to prediction of production carrying capacity in shellfish farming., in: Shumway, S. (Ed.), Shellfish Aquaculture and the Environment. Wiley-Blackwell Science Publishers, Ames, IA, pp. 135–

154.

Guyondet, T., Comeau, L. a., Bacher, C., Grant, J., Rosland, R., Sonier, R., Filgueira, R., 2014. Climate Change Influences Carrying Capacity in a Coastal Embayment Dedicated to Shellfish Aquaculture. Estuaries and Coasts 38, 1593–1618. https://doi.org/10.1007/s12237-014-9899-x

Guyondet, T., Roy, S., Koutitonsky, V.G., Grant, J., Tita, G., 2010. Integrating multiple spatial scales in the carrying capacity assessment of a coastal ecosystem for bivalve aquaculture. J. Sea Res. 64, 341–359. https://doi.org/10.1016/j.seares.2010.05.003

Harzallah, A., Chapelle, A., 2002. Influence de la variabilité climatique sur l' apparition de crises anoxiques ou 'malaïgues' dans l' étang de Thau (sud de la France). Oceanol. Acta 25, 79–86. https://doi.org/10.1016/s0399-1784(02)01184-2

Higgins, C.B., Stephenson, K., Brown, B.L., 2011. Nutrient Bioassimilation Capacity of Aquacultured Oysters: Quantification of an Ecosystem Service. J. Environ. Qual. 40, 271. https://doi.org/10.2134/jeq2010.0203

Jiang, W., Gibbs, M.T., 2005. Predicting the carrying capacity of bivalve shellfish culture using a steady, linear food web model. Aquaculture 244, 171–185. https://doi.org/10.1016/j.aquaculture.2004.11.050

Kashiwai, M., 1998. History of carrying capacity concept as an index of ecosystem productivity: (Review). Bull. Hokkaido Natl. Fish. Res. Inst. 59, 81–100.

Kellogg, M.L., Smyth, A.R., Luckenbach, M.W., Carmichael, R.H., Brown, B.L., Cornwell, J.C., Piehler, M.F., Owens, M.S., Dalrymple, D.J., Higgins, C.B., 2014. Use of oysters to mitigate eutrophication in coastal waters. Estuar. Coast. Shelf Sci. 151, 156–168. https://doi.org/10.1016/j.ecss.2014.09.025

Kooijman, S.A.L.M., 2010. Dynamic energy budget theory and population ecology: lessons from Daphnia. Philos. Trans. R. Soc. B Biol. Sci. 365, 3541–3552.

https://doi.org/10.1098/rstb.2010.0167

Kooijman, S.A.L.M., 2009. Dynamic Energy Budget Theory 514.

Lagarde, F., Fiandrino, A., Ubertini, M., D'Orbcastel, E.R., Mortreux, S., Chiantella, C., Bec, B., Bonnet, D., Roques, C., Bernard, I., Richard, M., Guyondet, T., Pouvreau, S., Lett, C., 2019. Duality of trophic supply and hydrodynamic connectivity drives spatial patterns of Pacific oyster recruitment. Mar. Ecol. Prog. Ser. https://doi.org/10.3354/meps13151

La Jeunesse, I., 2001. Etude intégrée dynamique du phosphore dans le système bassin versant-lagune de Thau.

La Jeunesse, I., Elliott, M., 2004. Anthropogenic regulation of the phosphorus balance in the Thau catchment-coastal lagoon system (Mediterraean Sea, France) over 24 years. Mar. Pollut. Bull. 48, 679–687. https://doi.org/10.1016/j.marpolbul.2003.10.011

McKindsey, C.W., Thetmeyer, H., Landry, T., Silvert, W., 2006. Review of recent carrying capacity models for bivalve culture and recommendations for research and management. Aquaculture 261, 451–462. https://doi.org/10.1016/j.aquaculture.2006.06.044

Ministère de l'Ecologie, du Développement Durable et de l'Energie (MEDDE), 2015. Arrêté du 27 juillet 2015 modifiant l'arrêté du 25 janvier 2010 relatif aux méthodes et critères d'évaluation de l'état écologique, de l'état chimique et du potentiel écologique des eaux de surface pris en application des articles R. 212-10, R. 212-11 et R. 212-18 du Code de l'Environnement. JORF n°0198, p. 15032. https://www.legifrance.gouv.fr/eli/arrete/2015/7/27/DEVL1513989A/jo/texte.

Nunes, J.P., Ferreira, J.G., Gazeau, F., Lencart-Silva, J., Zhang, X.L., Zhu, M.Y., Fang, J.G., 2003. A model for sustainable management of shellfish polyculture in coastal bays. Aquaculture 219, 257–277. https://doi.org/10.1016/S0044-8486(02)00398-8

Parsons, T.R., Stephens, K., Strickland, J.D.H., 1961. On the Chemical Composition of Eleven Species of Marine Phytoplankters. J . Fish . Res . Bd . Can . Downloaded from

1129 www.nrcresearchpress.com by WAGENINGEN UR on 09 / 08 / 15.
1130 Pernet, F., Barret, J., Le Gall, P., Corporeau, C., Dégremont, L., Lagarde, F., Pépin, J.F.,
1131 Keck, N., 2012. Mass mortalities of Pacific oysters *Crassostrea gigas* reflect infectious
1132 diseases and vary with farming practices in the Mediterranean Thau lagoon, France. Aquac.
1133 Environ. Interact. 2, 215–237. https://doi.org/10.3354/aei00041
1134 Platt, T., Irwin, B., 1973. Caloric content of phytoplankton. Limnol. Oceanogr. 18, 306–310.
1135 https://doi.org/10.4319/lo.1973.18.2.0306
1136 Plus, M., Jeunesse, I. La, Bouraoui, F., Zaldívar, J.M., Chapelle, A., Lazure, P., 2006.
1137 Modelling water discharges and nitrogen inputs into a Mediterranean lagoon: Impact on the
1138 primary production, in: Ecological Modelling. pp. 69–89.
1139 https://doi.org/10.1016/j.ecolmodel.2005.07.037
1140 Pouvreau, S., Bourles, Y., Lefebvre, S., Gangnery, A., Alunno-Bruscia, M., 2006. Application
1141 of a dynamic energy budget model to the Pacific oyster, *Crassostrea gigas*, reared under
1142 various environmental conditions. J. Sea Res. 56, 156–167.
1143 https://doi.org/10.1016/j.seares.2006.03.007
1144 Raillard O., Ménesguen A., 1994. An ecosystem box-model for estimating the carrying
1145 capacity of a macrotidal shellfish system. Mar.Ecol.Prog.Ser. 115, 117-130.
1146 REPHY. 2017. French Observation and Monitoring program for Phytoplankton and
1147 Hydrology in coastal waters. 1987-2016 Metropolitan data. SEANOE database
1148 (http://doi.org/10.17882/47248).
1149 Rose, J.M., Bricker, S.B., Ferreira, J.G., 2015. Comparative analysis of modeled nitrogen
1150 removal by shellfish farms. Mar. Pollut. Bull. 91, 185–190.
1151 https://doi.org/10.1016/j.marpolbul.2014.12.006
1152 Smaal, A.C., Prins, T.C., Dankers, N., Ball, B., 1997. Minimum requirements for modelling
1153 bivalve carrying capacity. Aquat. Ecol. 31, 423–428.

https://doi.org/10.1023/A:1009947627828

Soetaert, K., Petzoldt, T., Setzer, R.W., 2010. Package deSolve : Solving Initial Value Differential Equations in R. J. Stat. Softw. 33, 1–25.

Souchu, P., Bec, B., Smith, V.H., Laugier, T., Fiandrino, A., Benau, L., Orsoni, V., Collos, Y., Vaquer, A., 2010. Patterns in nutrient limitation and chlorophyll a along an anthropogenic eutrophication gradient in French Mediterranean coastal lagoons. Can. J. Fish. Aquat. Sci. 753, 743–753. https://doi.org/10.1139/F10-018

Souchu, P., Gasc, A., Collos, Y., Vaquer, A., Tournier, H., Bibent, B., Deslous-Paoli, J.M., 1998. Biogeochemical aspects of bottom anoxia in a Mediterranean lagoon (Thau, France). Mar. Ecol. Prog. Ser. 164, 135–146. https://doi.org/10.3354/meps164135

Troussellier, M., Deslous-Paoli, J.M., 2001. La lagune de Thau: un site atelier pour l'acquisition, l'intégration et la valorisation des connaissances. Oceanis 27, 257–289.

Willmott, C.J., 1981. On the validation of models. Phys. Geogr. 2, 184–194.